Minimal Matchings for dP3 Cluster Variables

Judy Chiang, Son Nguyen

August 5, 2022

Contents

1 Introduction

Upon Fomin and Zelvinsky's pioneer work [8][9] in cluster algebras for the study of total positivity and dual canonical bases in semisimple Lie groups, a great variety of its applications have been found in combinatorics, tropical geometry [5], Teichmüller theory [16], representation theory

[2]. With the introduction of Laurent phenomenon, mathematicians [15] [12] [3] have been intrigued to study combinatorial interpretations for the cluster variables as perfect matchings of graphs, under suitable weighting schemes . Of particular interest is the situation where the graphs are directly related to the quiver of the cluster algebra, namely when they are subgraphs of the dual of the quiver.

Previous work in dP3 quiver has considered both a single and an infinite class of mutation sequence on this quiver to a class of subgraphs of its brane tiling (known as Aztec dragons and Aztec castles respectively) [17] [12]. As Zhang [17] proved the explicit formula for cluster variables of Aztec dragon, Leoni-Musiker-Neel-Turner [13] proved a more generalized mutation sequence. Afterwards, Lai-Musiker [12] found explicit formula for cluster variables of Aztec castles with Aztec dragons as a special case.

Our paper is concerned with a variant of such quiver over the del Pezzo surface dP3, where we include a second alphabet of variables, $\{y_1, y_2, \ldots, y_n\}$, that breaks the symmetry of this recurrence. This deformation is motivated by the theory of cluster algebras with principal coefficients introduced by Fomin and Zelvinsky [9]. We attempt to answer Question 1 and our goal is to obtain combinatorial formulas for the Laurent expansions of cluster variables obtained by certain sequences of mutations of quivers of interest to string theorists such as those associated to reflexive polygons [1].

Question 1. *Given a deformation of the dP3 quiver with an infinite class of mutation sequence as introduced in [12], what is the combinatorial interpretations for the cluster variables? In other words, what is the minimal matching for an Aztec castle graph?*

Our main result is the construction of the minimal matching of Aztec Castles in Section 5.1 and the outline of the paper proceeds as follows. In Section 2, we discuss the backgrounds of quivers by reminding the readers definitions of quiver and cluster mutations in Section 2.1. Then, we introduce their deformations (framed quivers) in Section 2.6. Specifically, we introduce dP-3 quivers and the construction of Aztec castles described in [12] along with Aztec dragons as a special case. We give the construction of minimal matching of Aztec Castles in Section 5 and discuss the proof of Theorem 5.1 in Section 6.

2 Background

2.1 Quiver and cluster mutations

A **quiver** Q is a directed finite graph with a set of vertices V and a set of directed edges E connecting them such that there are no loops or 2-cycles. We can relate a **cluster algebra** with **initial seed** $\{x_1, x_2, \ldots, x_n\}$ to Q by associating a cluster variable x_i to every vertex labeled i in Q where $|V| = n$. The **cluster** is the union of the cluster variables at each vertex.

Definition 2.1. **[Quiver Mutation** [8]] Mutating at a vertex i in Q is denoted by μ_i and corresponds to the following actions on the quiver:

- For every 2-path through i (e.g. $j \to i \to k$), add an edge from j to k.
- Reverse the directions of the arrows incident to i
- Delete any 2-cycles created from the previous two steps.

When we mutate at a vertex i, the cluster variable at this vertex is updated and all other cluster variables remain unchanged. The action of μ_i on the cluster leads to the following binomial exchange relation:

$$x_i' x_i = \prod_{i \to j \text{ in } Q} x_j^{a_{i\to j}} + \prod_{j \to i \text{ in } Q} x_j^{b_{j\to i}}$$

where x_i' is the new cluster variable at vertex i, $a_{i\to j}$ denotes the number of edges from i to j, and $b_{j\to i}$ denotes the number of edges from j to i.

It was proved in [8] that every cluster variable is a *Laurent polynomial* in $\mathbb{Z}[x_1, \ldots, x_n]$, i.e.

$$x_m = \frac{P(x_1, \ldots, x_n)}{x_1^{d_1} \ldots x_n^{d_n}}$$

for all m.

2.2 del Pezzo 3 quiver and lattice

Our focus on this project is the del Pezzo 3 (dP3) quiver illustrated in Figure 1. By unfolding this quiver, we get the infinite unfolded dP3 quiver as shown in Figure 2. Then, taking the dual graph of the unfolded quiver yields its brane tiling in Figure 3, which will be referred to as the **dP3 lattice**. The notion of brane tiling is first introduced in physics but later interpreted by Cottrell-Young [4] as a version of the domino shuffling algorithm. This doubly periodic, bipartite, planar graphs arise in string theory where theoretical physicist can associate an infinite class of supersymmetric quiver gauge theories to a corresponding toric variety (which is a Calabi–Yau 3-fold) as well as this combinatorial model. They appear physically in string theory through the intersections of NS5 and D5-branes which are dual to a configuration of D3-branes probing the singularity of a toric Calabi–Yau threefold [7]. Because of its geometry connection and how the $(3 + 1)$ dimensional supersymmetric gauge field theory lives on the worldvolume of the D3-brane, it can be represented by the **dP3 quiver**.

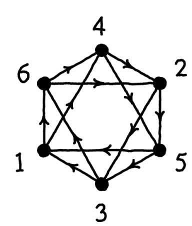

Figure 1: dP3 quiver

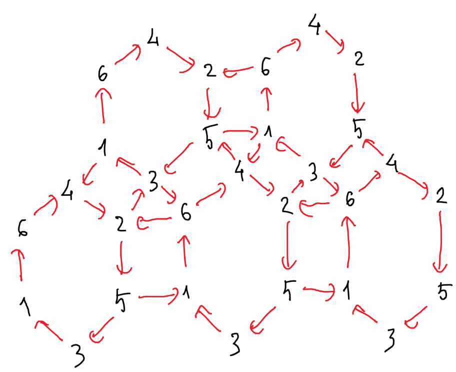

Figure 2: Unfolded dP3 quiver

2.3 Toric mutations and prism walk

2.3.1 Toric mutations

A vertex is **toric** if its in-degree and out-degree are both 2. A **toric mutation** is a mutation at a toric vertex. In this paper, we will study the following five actions on the dP3 quiver, which are also

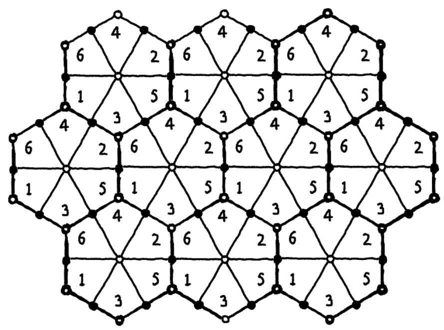

Figure 3: dP3 lattice

the main actions studied in [12].

Definition 2.2. Define the following actions

$$\tau_1 = \mu_1 \circ \mu_2 \circ (12),$$

$$\tau_2 = \mu_3 \circ \mu_4 \circ (34),$$

$$\tau_3 = \mu_5 \circ \mu_6 \circ (56),$$

$$\tau_4 = \mu_1 \circ \mu_4 \circ \mu_1 \circ \mu_5 \circ \mu_1 \circ (145),$$

$$\tau_5 = \mu_2 \circ \mu_3 \circ \mu_2 \circ \mu_6 \circ \mu_2 \circ (236),$$

where we apply a graph automorphism of Q and permutation to the labeled seed after the sequence of mutations.

One can then check that on the level of quivers and labeled seeds (i.e. ordered clusters), we have the following identities, which are also noted in [12]: For all i, j such that $1 \leq i \neq j \leq 3$, we have

$$\begin{gathered}
\tau_1(Q) = \tau_2(Q) = \tau_3(Q) = \tau_4(Q) = \tau_5(Q) = Q \\
(\tau_i)^2\{x_1, x_2 \ldots, x_6\} = (\tau_4)^2\{x_1, x_2 \ldots, x_6\} = (\tau_5)^2\{x_1, x_2 \ldots, x_6\} = \{x_1, x_2 \ldots, x_6\} \\
(\tau_i\tau_j)^3\{x_1, x_2 \ldots, x_6\} = \{x_1, x_2 \ldots, x_6\}, \\
\tau_i\tau_4\{x_1, x_2 \ldots, x_6\} = \tau_4\tau_i\{x_1, x_2 \ldots, x_6\}, \\
\tau_i\tau_5\{x_1, x_2 \ldots, x_6\} = \tau_5\tau_i\{x_1, x_2 \ldots, x_6\}.
\end{gathered}$$

2.3.2 Prism walk

We will model the mutations in defined in Definition 2.2 as prism walk on a square triangulated lattice, illustrated in Figure 4b. We will place the prism so that the coordinates of vertices $1, \ldots, 6$ are $(0, -1, 1), (0, -1, 0), (-1, 0, 0), (-1, 0, 1), (0, 0, 1), (0, 0, 0)$ respectively. The reason is the cluster variables corresponding to these coordinates, described in Section 2.4, are $x_1, \ldots, x_6$ respectively.

Figure 5 and 6 show how τ_1 and τ_4 act on the prism. Thus, τ_1, τ_2, τ_3 correspond to reflecting the prism about its three side faces, as illustrated in Figure 7, while τ_4, τ_5 correspond to reflecting the prism about its two top faces, as in Figure 8.

One can check that using these five τ-mutations, we can indeed move the original prism to any isometric prism in the $\mathbb{Z}^3$ lattice. Conversely, any sequence of τ-mutations can be modeled as a prism in the $\mathbb{Z}^3$ lattice. As a result, we can associate a cluster variable $z_{i,j,k}$ to each point (i, j, k) in $\mathbb{Z}^3$.

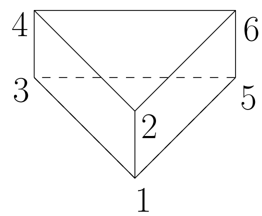

(a) Prism

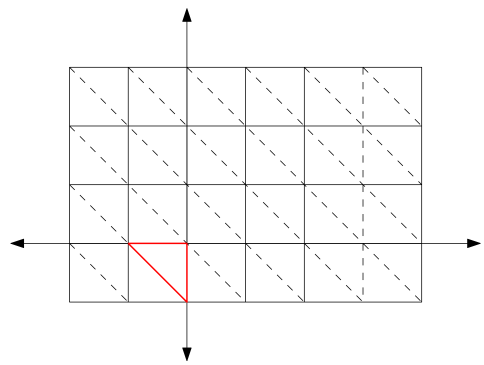
(b) Lattice

Figure 4: Prism and lattice

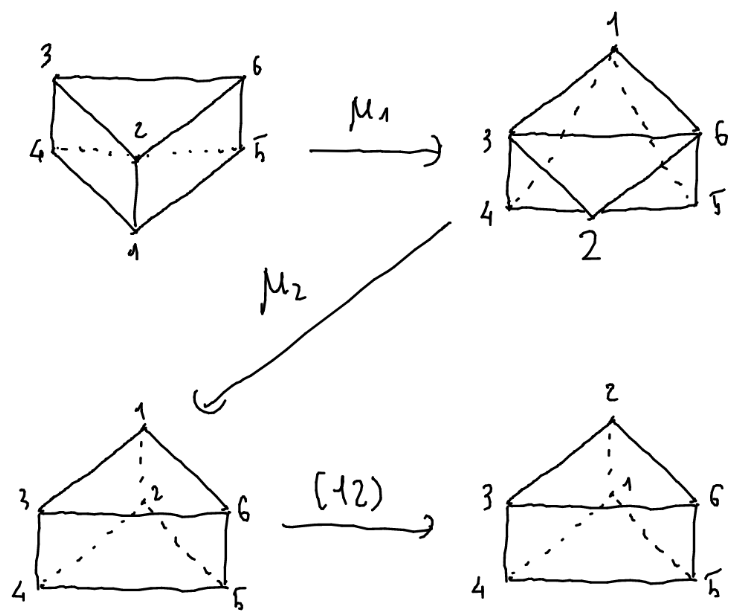

Figure 5: τ_1 action on the prism

2.4 Aztec Castles

2.4.1 Construction

In this section, we describe the construction of **Aztec Castles** from the points in the $\mathbb{Z}^3$ lattice as this will give the cluster variables for the τ-mutations. In general, the construction of Aztec Castles consists of the following steps, as described in [12].

- *Step 1:* We start with a 6-tuple $(a, b, c, d, e, f) \in \mathbb{Z}^6$ and draw a **(six-sided) contour** $\mathcal{C}(a, b, c, d, e, f)$ on the dP3 lattice in the direction in Figure 9. We start from a vertex in the center of a hexagon, and define the unit length to be two "long" edges of the lattice. Note that if an element of the tuple is 0, we simply skip the corresponding side, and if an element is negative, we transverse in the opposite direction.

  Also note that we want to pick a 6-tuple so that the resulting contour is closed. We will ex-

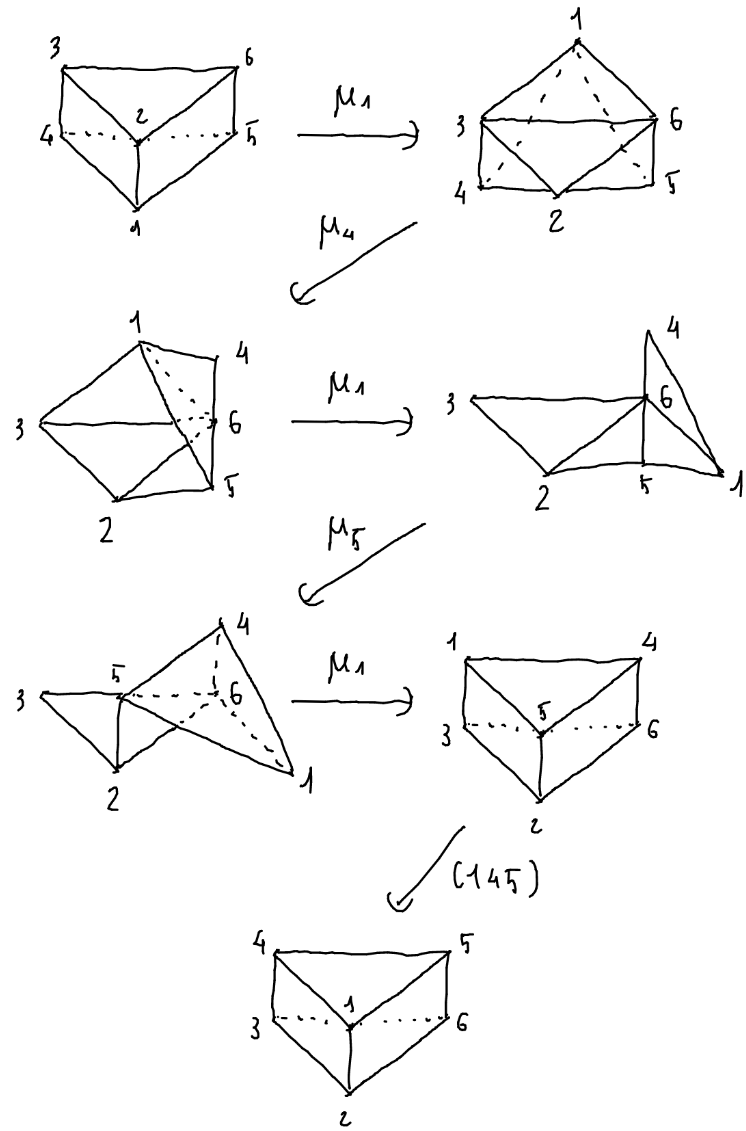

Figure 6: τ_4 action on the prism

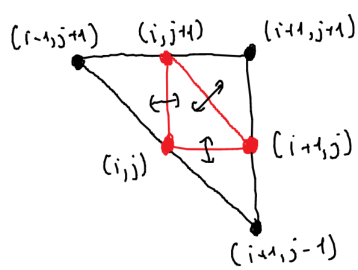

Figure 7: Three reflections corresponding to τ_1, τ_2, τ_3

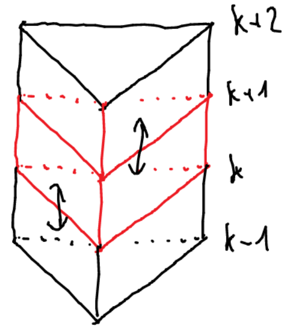

Figure 8: Two reflections corresponding to τ_4, τ_5

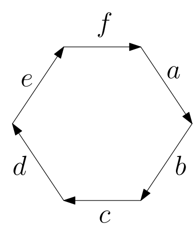

Figure 9: Contour direction

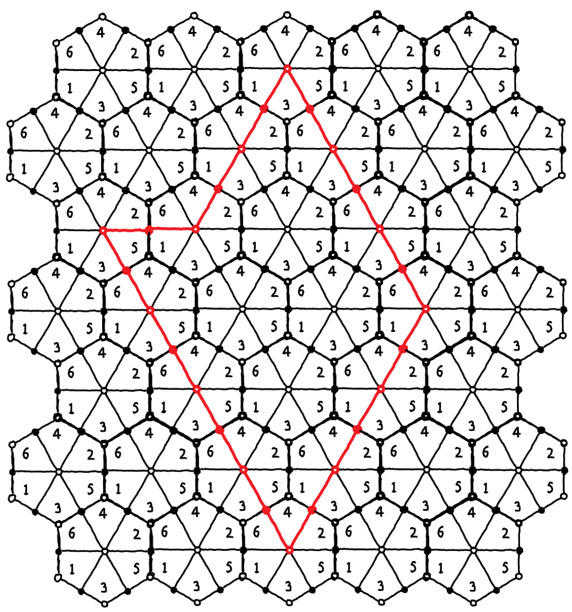

Figure 10: Step 1

plain this further in Section 2.4.2. Figure 10 shows an example of a contour when the tuple is $(4, -3, 0, 3, -2, -1)$.

- *Step 2:* We remove every vertex outside the contour and keep only the vertices inside, as in Figure 11.

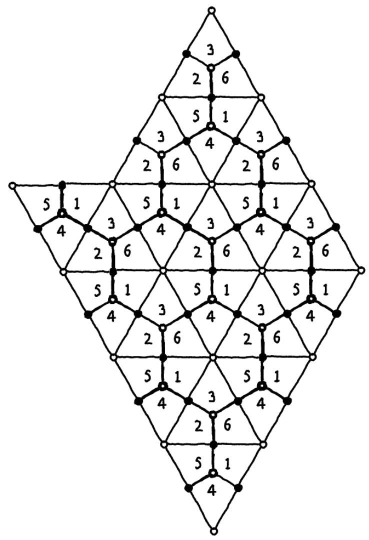

Figure 11: Step 2

- *Step 3:* We remove vertices along the sides as follow. For any side of positive (resp. negative) length, we remove all black (resp. white) vertices along that side. For any side of length zero, this side corresponds to a single vertex. If any of the adjacent sides is negative, then this vertex is already removed. If this side is between two sides of length zero, we will also remove this vertex. The only case that we keep this vertex is when it is between two sides of positive lengths. Figure 12 shows the resulting graph after this step.

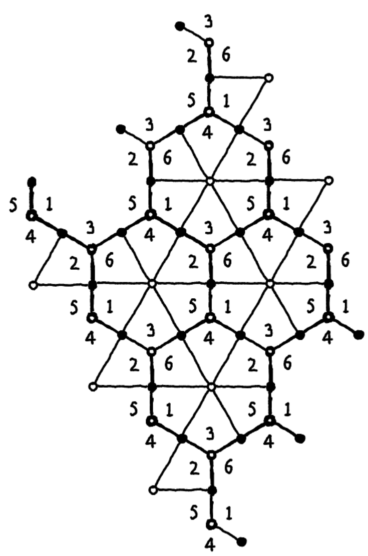

Figure 12: Step 3

- *Step 4:* Finally, we have some "dangling" edges, which are edges in which one of the two incident vertices has degree 1. These are the red edges in Figure 13. For these edges, we can either keep or remove the two incident vertices. The reason is that when considering perfect matchings of this graph, these edges are always forced to be in the matching, and they do not contribute to the weight of the matching (which will be defined in Section 2.4.3). For this paper, we opt to keep these edges.

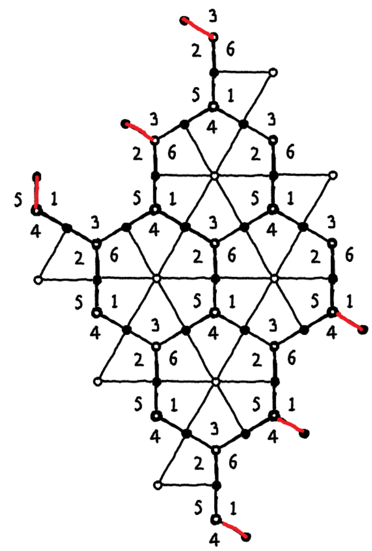

Figure 13: Step 4

The resulting graph after the above four steps is an Aztec Castle.

2.4.2 Contour parametrization

We now discuss the requirements we have for the 6-tuple as described in lemma 5.3 of [12]. First of all, for the contour to be closed, we want

$$a+b=d+e \quad \text{and} \quad c+d=f+a.$$

We also want $b+c=e+f$, but this is implied by the above two relations, so we do not include this condition. Finally, since we will work with perfect matchings of this graph, we want the same number of white vertices and black vertices. By counting the number of vertices deleted on each side in step 3 of the construction, Lai and Musiker introduced a third condition which allows for an equal number of black and white vertices:

$$a+b+c+d+e+f=1.$$

With these three conditions, we can parametrize the 6-tuple by three parameters as follows.

Definition 2.3. Define the Castle $\mathcal{C}_{i,j,k}$ to be the Castle constructed by the contour

$$\mathcal{C}(j+k,-i-j-k,i+k,j+1-k,-i-j-1+k,i+1-k)$$

One can check that the above tuple satisfies all three aforementioned conditions. Thus, we can associate each point in $\mathbb{Z}^3$ to an Aztec Castle. Different possible shapes of Aztec Castles can be seen in figures 14 and 15. There are also degenerate cases at the lines separating the regions where one or two sides have length 0. We number the cases as in the two figures, leaving out the yellow region since the contour in that case has a self-intersection, and we do not have a full understanding of that type of Castle yet.

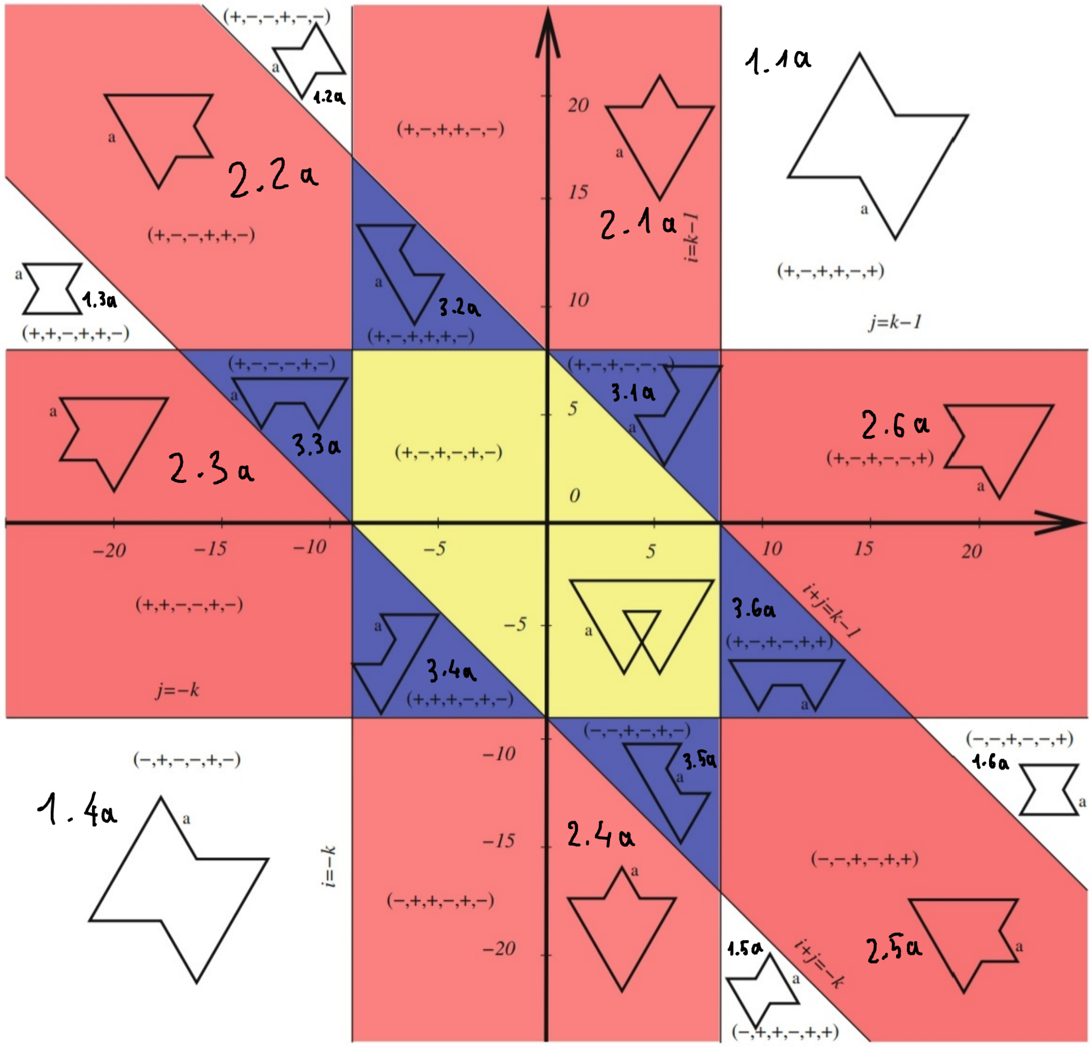

Figure 14: Possible Castle shapes for a fixed $k \geq 1$, source: [12]

2.4.3 Weight

For every Aztec Castle $C_{i,j,k}$, we will use the common definition of the weight of a perfect matching m as defined by Speyer in [15].

$$wt(m) = \begin{cases} \prod\limits_{f \in G_{t+1}} x_f^{(s-1)-|E(f) \cap m|}, \text{ if } f \in G^{\circ} \\ \prod\limits_{f \in G_{t+1}} x_f^{\lfloor \frac{s}{2} \rfloor - |E(f) \cap m|}, \text{ if } f \in \partial G \end{cases},$$

where G is the graph, and f is a face of a $2s-$gon in the graph.

In our discussion of Aztec Castles, since all faces are 4-gons, the formula for the weight can be simplified to

$$wt(m) = \prod_{f \in G_{t+1}} x_f^{(1-|E(f) \cap m|)}.$$

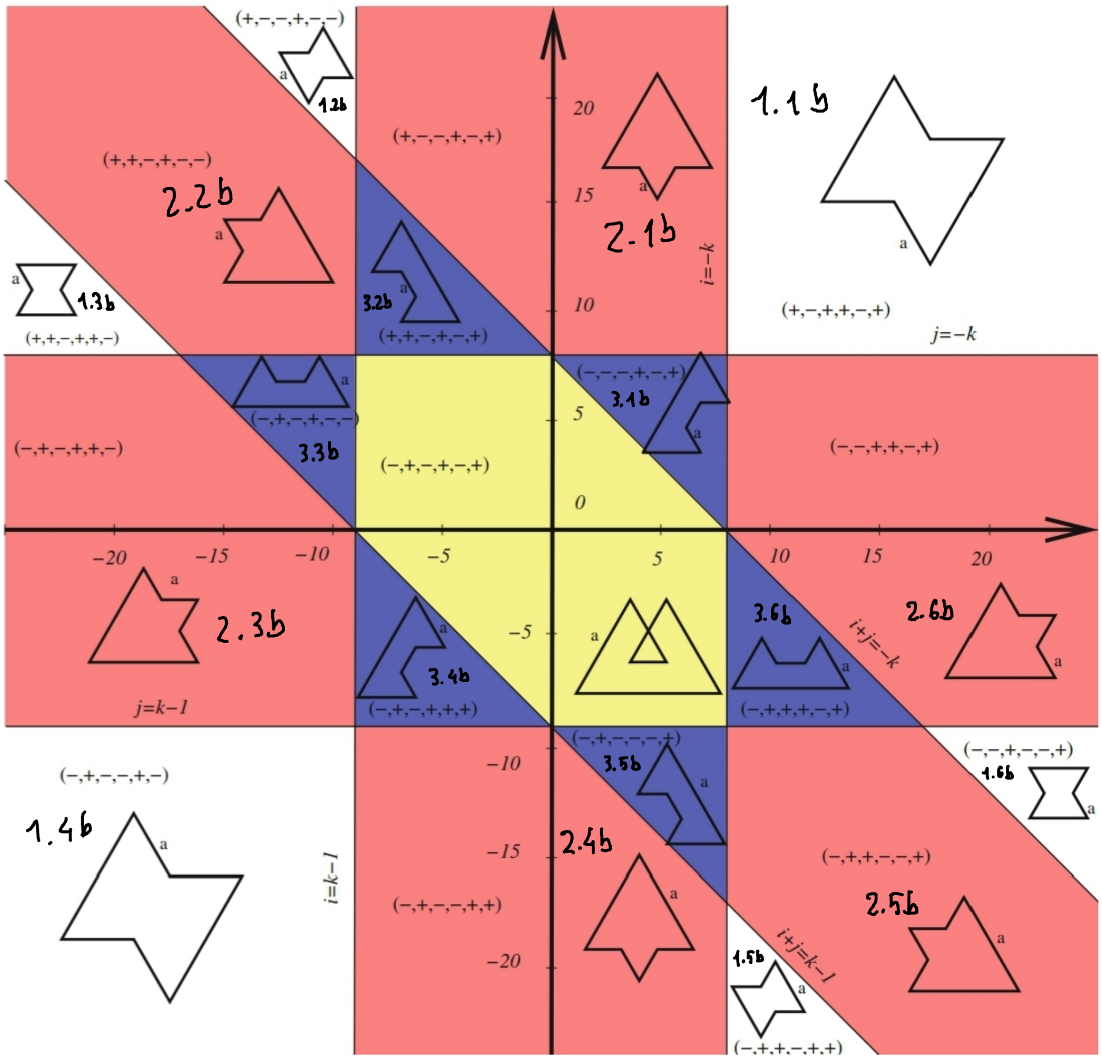

Figure 15: Possible Castle shapes for a fixed $k \leq 0$, source: [12]

With the weight of each perfect matching defined, we have the following definition of the weight of an Aztec Castle:

$$wt(C_{i,j,k}) = \sum_{m} wt(m).$$

Lai and Musiker [12] prove the following theorem about Aztec Castle.

Theorem 2.1. *Let $z_{i,j,k}$ be the cluster variable at point (i,j,k). Then if (i,j,k) is not in the yellow region in Figure 14 and 15, we have*

$$z_{i,j,k} = wt(C_{i,j,k}).$$

2.5 Aztec Dragons

A special family of Aztec Castles is the family of Aztec Dragons, which are Aztec Castles with $i \in \{-1, 0\}, k \in \{0, 1\}$, and $j \geq 0$. Specifically, we define D_n to be $C_{0,n,1}$ and $D_{n+1/2}$ to be $C_{-1,n+1,0}$. Also, we define D'_n to be $C_{0,n,0}$ and $D'_{n+1/2}$ to be $C_{-1,n+1,1}$. Some examples of Aztec Dragons can be seen in figures 16 and 17. Notice that D'_n is a 180° rotation of D_n, and $D'_{n+1/2}$ is a 180° rotation of $D_{n+1/2}$. It was proved in [17] that the weights of Aztec Dragons are the cluster variables of the dP3 quiver after mutations $\tau_1\tau_2\tau_3\tau_1\tau_2\tau_3\ldots$

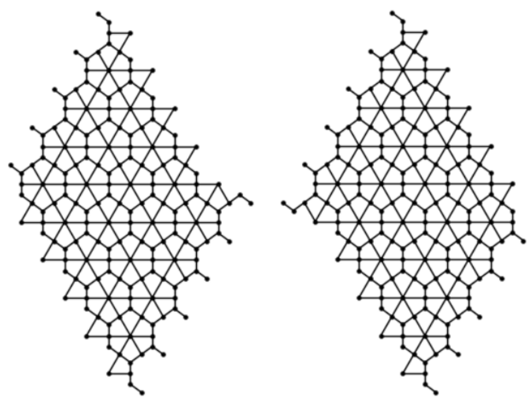

Figure 16: Aztec Dragons D_5 and D'_5

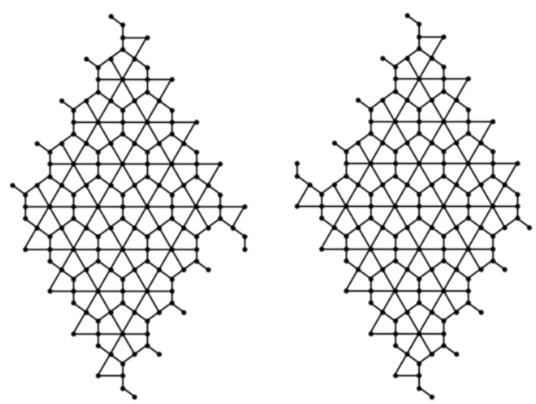

Figure 17: Aztec Dragons $D_{4+1/2}$ and $D'_{4+1/2}$

2.6 Framed quiver, c-vector, g-vector and F-polynomial

2.6.1 Framed quiver and c-vector

For a quiver Q, the associated **framed quiver** $\hat{Q}$ is a directed graph in which

$$V_{\hat{Q}} = V_Q \cup \{v_{i+n} \mid v_i \in V_Q\} \quad \text{and} \quad E_{\hat{Q}} = E_Q \cup \{v_i \to v_{i+n} \mid v_i \in V_Q\}.$$

The additional vertices in $\hat{Q}$ are called *frozen vertices*, which means that we never mutate at these vertices. An important family of integer vectors relating to the framed quiver, called **c-vectors**, was introduced in [9].

Definition 2.4. Let B be the incidence matrix of $\hat{Q}$. Then for each $\ell = 1, \dots, n$, the **c-vector** c_ℓ is defined to be $c_\ell = (b_{n+1,\ell}, \dots, b_{2n,\ell})^T$.

A key property of c-vectors is *sign-coherence*, which means that all entries in each c-vector is either nonnegative or nonpositive. This was conjectured in [9] and first proved for quivers in [6]. The general case for cluster was proved in [10].

2.6.2 F-polynomial and g-vector

We also associate new cluster variables $\{y_1, \dots, y_n\}$ to the frozen vertices. Then every cluster variable is a *Laurent polynomial* in $\mathbb{Z}[x_1, \dots, x_n, y_1, \dots, y_n]$, i.e.

$$x_m = \frac{P(x_1, \dots, x_n, y_1, \dots, y_n)}{x_1^{d_1} \dots x_n^{d_n}}$$

for all m. These are called the **principal coefficients** of the cluster variable.

Setting $x_1 = \dots = x_n = 1$, we obtain the **F-polynomial** of the cluster variable, i.e. we have

$$F_m = P(1, \dots, 1, y_1, \dots, y_n).$$

As a corollary of the *sign-coherence* property of c-vectors, the F-polynomial always contains a unique term 1 (Proposition 5.6 in [9]). This means that there is a unique term in x_m in which the exponents of y_i is 0 for all i, in other words, this term is a monomial in $\mathbb{Z}[x_1, \dots, x_n]$. We will refer to this as the **minimal monomial** of x_m.

The minimal monomials form another prominent family of integer vectors introduced in [9] called the **g-vectors**.

Definition 2.5. Let $x_1^{g_1} \dots x_n^{g_n}$ be the minimal monomial of x_m. Then the **g-vector** c_m is defined to be $c_m = (g_1, \dots, g_n)$.

Since the Laurent polynomial of any x_m is homogeneous, if we set

$$y_i = \frac{\prod_{\text{edge } j \to i} x_j}{\prod_{\text{edge } i \to j} x_j}$$

for all i, then the resulting polynomial consists of a single term whose exponents are the g-vector. Therefore, finding the F-polynomial is sufficient to find the Laurent polynomial (Proposition 6.3 in [9]). In the context of framed quiver, given Theorem 2.1, the cluster variable with principal coefficients are expected to be generating functions (or termed weighted sums) over the perfect matching for the Aztec castle. In this case, instead of simply taking the **weight** defined in Section 2.4.3, we also need to introduce the notion of **height** for each perfect matching. Then, based on Section 2.6.2, it is sufficient to define the minimal matching and show that its weight matched the g-vectors as desired.

Definition 2.6. The height $\mathsf{ht}(m) = f$, where f is the face in a closed loop created by superimposing the perfect matching m with the minimal matching.

2.6.3 c-matrix and g-matrix

Let the **c-matrix** C be the matrix whose columns are c-vectors, and **g-matrix** G be the matrix whose rows are g-vectors. We have the following theorem, which is a special case of a theorem proved in [14].

Theorem 2.2. *For any skew-symmetric exchange matrix B, we have*

$$G = (-C)^{-1}$$

Thus, we can find one matrix from the other.

3 Kuo condensation

Kuo condensation is the main tool of this paper. It was introduced by Kuo in [11], and can be considered a combinatorial interpretation of Dodgson condensation on determinants of matrices. Several versions of Kuo condensation were presented in [11], here we opt to state the versions that we will use in Section 6.

Lemma 3.1 (Balanced Kuo Condensation; Theorem 5.1 in [11])**.** *Let $G = (V_1, V_2, E)$ be a (weighted) planar bipartite graph with $|V_1| = |V_2|$. Assume that p_1, p_2, p_3, p_4 are four vertices appearing in a cyclic order on a face of G. Assume in addition that $p_1, p_3 \in V_1$ and $p_2, p_4 \in V_2$. Then*

$$\begin{aligned} w(G)w(G - \{p_1, p_2, p_3, p_4\}) =& w(G - \{p_1, p_2\})w(G - \{p_3, p_4\}) \\ &+ w(G - \{p_1, p_4\})w(G - \{p_2, p_3\}). \end{aligned} \tag{1}$$

Lemma 3.2 (Non-alternating Kuo Condensation; Theorem 5.3 in [11])**.** *Let $G = (V_1, V_2, E)$ be a planar bipartite graph with $|V_1| = |V_2|$. Assume that p_1, p_2, p_3, p_4 are four vertices appearing in a cyclic order on a face of G. Assume in addition that $p_1, p_2 \in V_1$ and $p_3, p_4 \in V_2$. Then*

$$\begin{aligned} w(G - \{p_1, p_4\})w(G - \{p_2, p_3\}) =& w(G)w(G - \{p_1, p_2, p_3, p_4\}) \\ &+ w(G - \{p_1, p_3\})w(G - \{p_2, p_4\}). \end{aligned} \tag{2}$$

We will now give a summary of how to pick the four points for Kuo condensation as presented in [12].

First, we define the points A, B, C, D, E, F on the sides a, b, c, d, e, f depending on the sign of each side, as shown in figures 18 and 19.

Deletion of these points yield forced edges as in figures 20 and 21. Therefore, the subgraph after removing A corresponds to the contour $C(a - 1, b + 1, c, d, e, f + 1)$ if A is black and to the contour $C(a + 1, b - 1, c, d, e, f - 1)$ if A is white. Analogous results hold for B, C, D, E, F. Thus, given an appropriate subgraph of a Castle, we can determine the right choice of four out of six points A, B, C, D, E, F based on the difference $(d_A, d_B, d_C, d_D, d_E, d_F)$ so that the subgraph after removing the four points is the desired subgraph.

4 Minimal matching of Aztec Dragons

We now gives the minimal matching of Aztec Dragons. Although this section is subsumed by Theorem 5.1 in Section 5, since Aztec Dragons are special cases of Aztec Castles, we think that this section is a great example for the general Aztec Castles.

4.1 C-matrix

Lemma 4.1. *Let C_i be the c-matrix of the quiver after the ith mutation in the sequence*

$$\mu_1\mu_2\mu_3\mu_4\mu_5\mu_6\mu_1\mu_2\mu_3\mu_4\mu_5\mu_6 \ldots,$$

then C_i has the following formula.

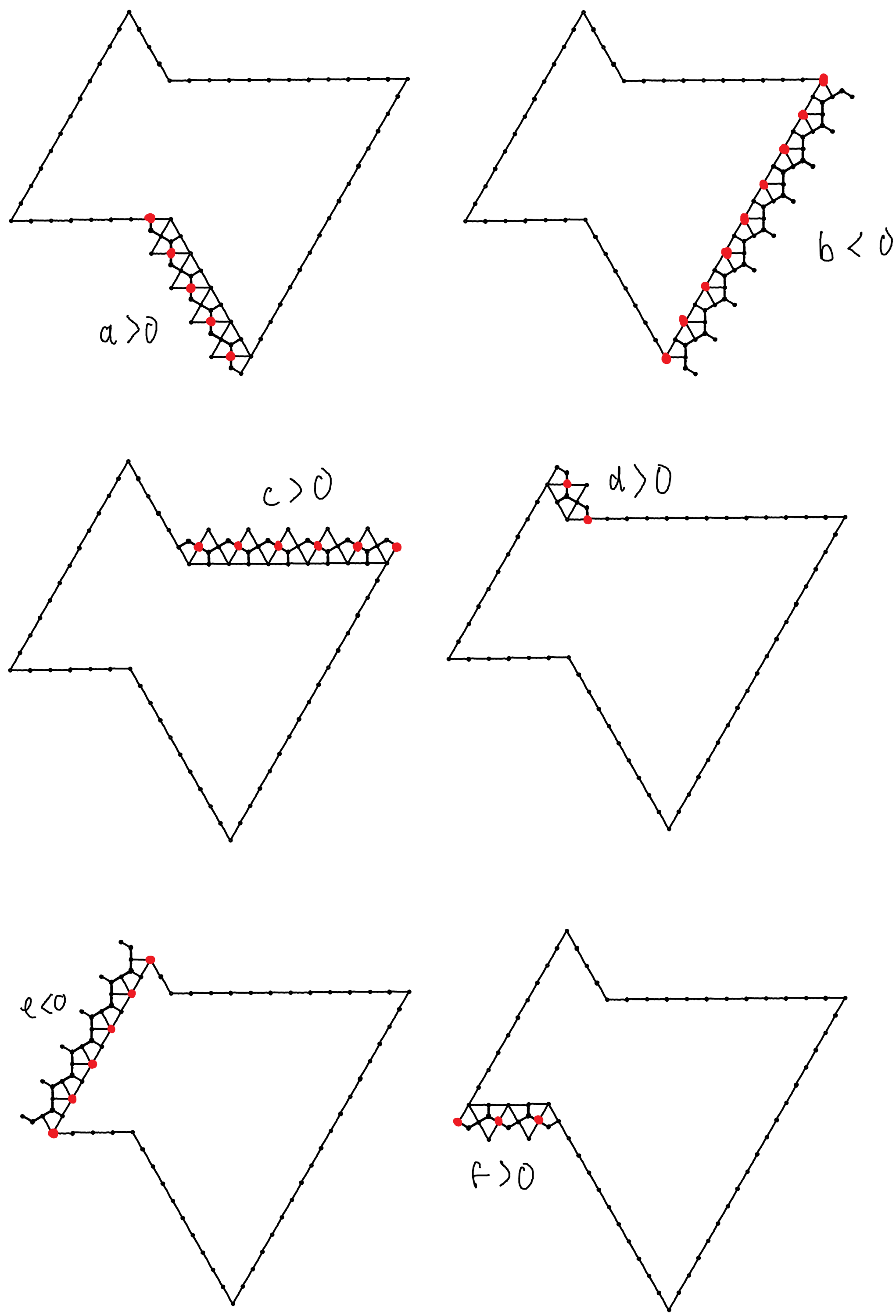

Figure 18: Choices of A, B, C, D, E, F when the signs are $+, -, +, +, -, +$

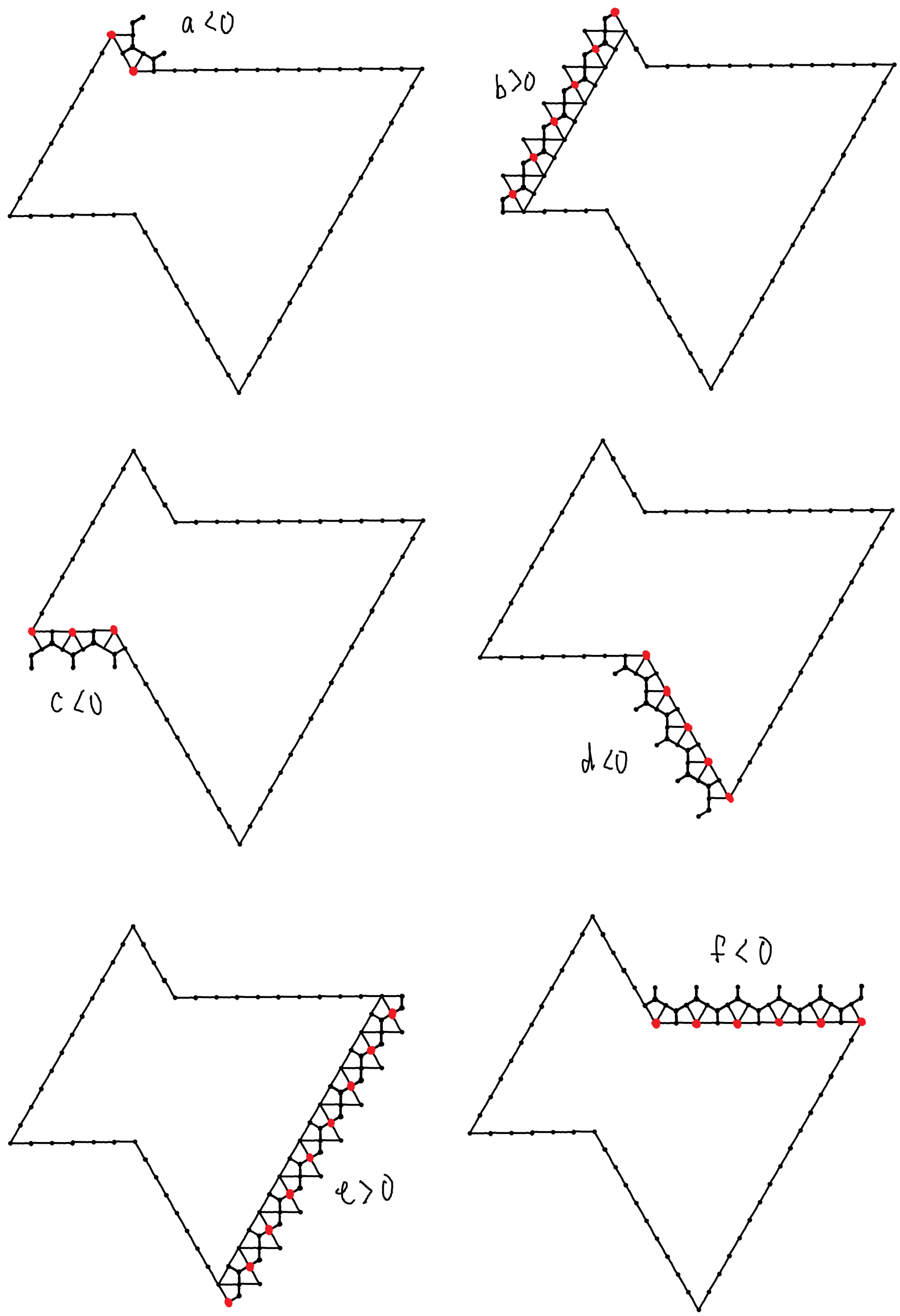

Figure 19: Choices of A, B, C, D, E, F when the signs are $-, +, -, -, +, -$

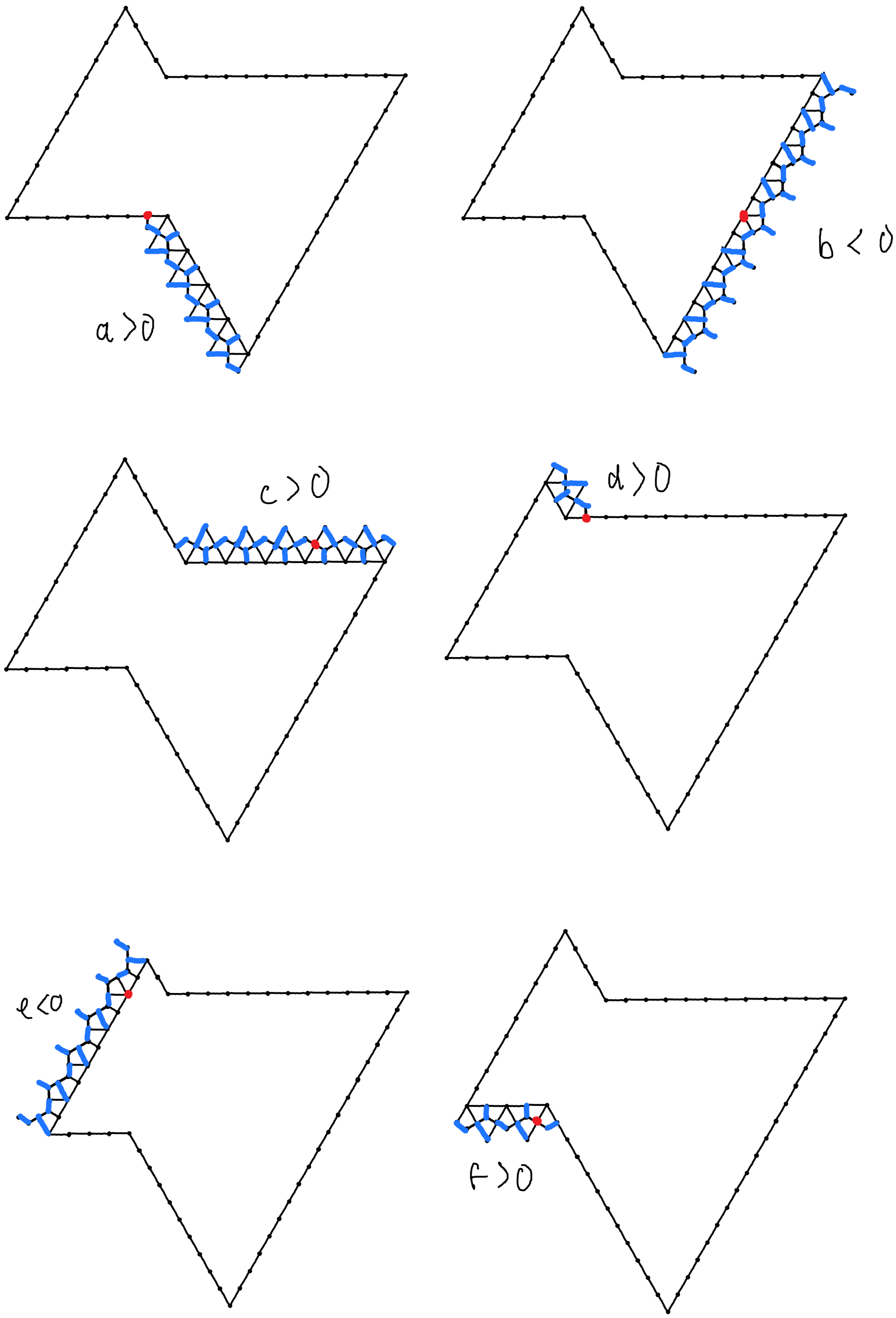

Figure 20: Deletion of A, B, C, D, E, F yields forced edges

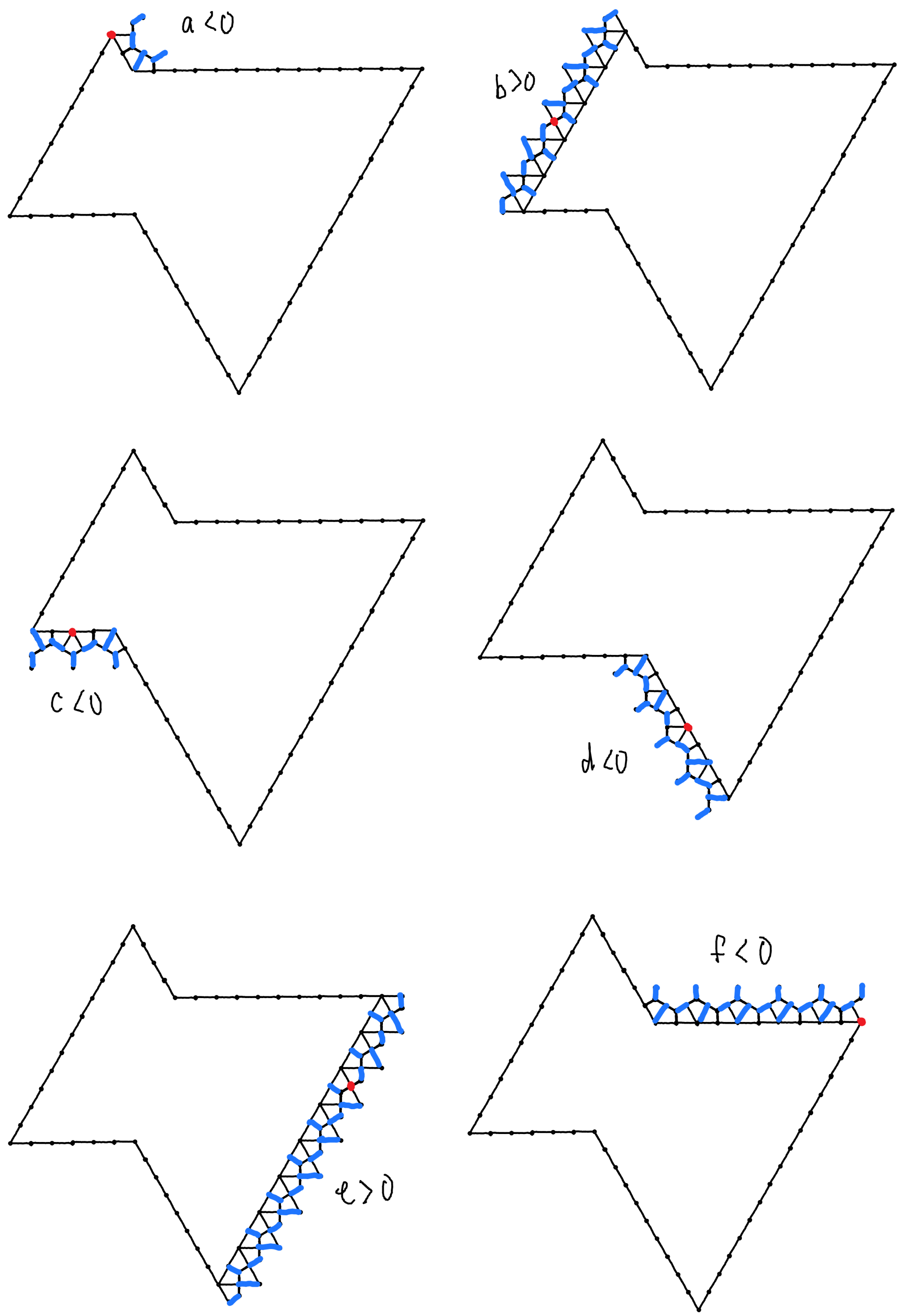

Figure 21: Deletion of A, B, C, D, E, F yields forced edges

$$Q_{0+12k} = \begin{bmatrix} -3k-1 & 0 & 0 & 0 & 3k & 0 \\ 0 & -3k-1 & 0 & 0 & 0 & 3k \\ -3k & 0 & -1 & 0 & 3k & 0 \\ 0 & -3k & 0 & -1 & 0 & 3k \\ -3k & 0 & 0 & 0 & 3k-1 & 0 \\ 0 & -3k & 0 & 0 & 0 & 3k-1 \end{bmatrix}, \qquad Q_{1+12k} = \begin{bmatrix} 3k+1 & 0 & -3k-1 & 0 & -1 & 0 \\ 0 & -3k-1 & 0 & 0 & 0 & 3k \\ 3k & 0 & -3k-1 & 0 & 0 & 0 \\ 0 & -3k & 0 & -1 & 0 & 3k \\ 3k & 0 & -3k & 0 & -1 & 0 \\ 0 & -3k & 0 & 0 & 0 & 3k-1 \end{bmatrix},$$

$$Q_{2+12k} = \begin{bmatrix} 3k+1 & 0 & -3k-1 & 0 & -1 & 0 \\ 0 & 3k+1 & 0 & -3k-1 & 0 & -1 \\ 3k & 0 & -3k-1 & 0 & 0 & 0 \\ 0 & 3k & 0 & -3k-1 & 0 & 0 \\ 3k & 0 & -3k & 0 & -1 & 0 \\ 0 & 3k & 0 & -3k & 0 & -1 \end{bmatrix}, \qquad Q_{3+12k} = \begin{bmatrix} 0 & 0 & 3k+1 & 0 & -3k-2 & 0 \\ 0 & 3k+1 & 0 & -3k-1 & 0 & -1 \\ -1 & 0 & 3k+1 & 0 & -3k-1 & 0 \\ 0 & 3k & 0 & -3k-1 & 0 & 0 \\ 0 & 0 & 3k & 0 & -3k-1 & 0 \\ 0 & 3k & 0 & -3k & 0 & -1 \end{bmatrix},$$

$$Q_{4+12k} = \begin{bmatrix} 0 & 0 & 3k+1 & 0 & -3k-2 & 0 \\ 0 & 0 & 0 & 3k+1 & 0 & -3k-2 \\ -1 & 0 & 3k+1 & 0 & -3k-1 & 0 \\ 0 & -1 & 0 & 3k+1 & 0 & -3k-1 \\ 0 & 0 & 3k & 0 & -3k-1 & 0 \\ 0 & 0 & 0 & 3k & 0 & -3k-1 \end{bmatrix}, \qquad Q_{5+12k} = \begin{bmatrix} -3k-2 & 0 & -1 & 0 & 3k+2 & 0 \\ 0 & 0 & 0 & 3k+1 & 0 & -3k-2 \\ -3k-2 & 0 & 0 & 0 & 3k+1 & 0 \\ 0 & -1 & 0 & 3k+1 & 0 & -3k-1 \\ -3k-1 & 0 & -1 & 0 & 3k+1 & 0 \\ 0 & 0 & 0 & 3 & 0 & -3k-1 \end{bmatrix},$$

$$Q_{6+12k} = \begin{bmatrix} -3k-2 & 0 & -1 & 0 & 3k+2 & 0 \\ 0 & -3k-2 & 0 & -1 & 0 & 3k+2 \\ -3k-2 & 0 & 0 & 0 & 3k+1 & 0 \\ 0 & -3k-2 & 0 & 0 & 0 & 3k+1 \\ -3k-1 & 0 & -1 & 0 & 3k+1 & 0 \\ 0 & -3k-1 & 0 & -1 & 0 & 3k+1 \end{bmatrix}, \qquad Q_{7+12k} = \begin{bmatrix} 3k+2 & 0 & -3k-3 & 0 & 0 & 0 \\ 0 & -3k-2 & 0 & -1 & 0 & 3k+2 \\ 3k+2 & 0 & -3k-2 & 0 & -1 & 0 \\ 0 & -3k-2 & 0 & 0 & 0 & 3k+1 \\ 3k+1 & 0 & -3k-2 & 0 & 0 & 0 \\ 0 & -3k-1 & 0 & -1 & 0 & 3k+1 \end{bmatrix},$$

$$Q_{8+12k} = \begin{bmatrix} 3k+2 & 0 & -3k-3 & 0 & 0 & 0 \\ 0 & 3k+2 & 0 & -3k-3 & 0 & 0 \\ 3k+2 & 0 & -3k-2 & 0 & -1 & 0 \\ 0 & 3k+2 & 0 & -3k-2 & 0 & -1 \\ 3k+1 & 0 & -3k-2 & 0 & 0 & 0 \\ 0 & 3k+1 & 0 & -3k-2 & 0 & 0 \end{bmatrix}, \qquad Q_{9+12k} = \begin{bmatrix} -1 & 0 & 3k+3 & 0 & -3k-3 & 0 \\ 0 & 3k+2 & 0 & -3k-3 & 0 & 0 \\ 0 & 0 & 3k+2 & 0 & -3k-3 & 0 \\ 0 & 3k+2 & 0 & -3k-2 & 0 & -1 \\ -1 & 0 & 3k+2 & 0 & -3k-2 & 0 \\ 0 & 3k+1 & 0 & -3k-2 & 0 & 0 \end{bmatrix},$$

$$Q_{10+12k} = \begin{bmatrix} -1 & 0 & 3k+3 & 0 & -3k-3 & 0 \\ 0 & -1 & 0 & 3k+3 & 0 & -3k-3 \\ 0 & 0 & 3k+2 & 0 & -3k-3 & 0 \\ 0 & 0 & 0 & 3k+2 & 0 & -3k-3 \\ -1 & 0 & 3k+2 & 0 & -3k-2 & 0 \\ 0 & -1 & 0 & 3k+2 & 0 & -3k-2 \end{bmatrix}, \qquad Q_{11+12k} = \begin{bmatrix} -3k-4 & 0 & 0 & 0 & 3k+3 & 0 \\ 0 & -1 & 0 & 3k+3 & 0 & -3k-3 \\ -3k-3 & 0 & -1 & 0 & 3k+3 & 0 \\ 0 & 0 & 0 & 3k+2 & 0 & -3k-3 \\ -3k-3 & 0 & 0 & 0 & 3k+2 & 0 \\ 0 & -1 & 0 & 3k+2 & 0 & -3k-2 \end{bmatrix}.$$

Proof. This can be easily proved by induction, noticing that

$$Q_0 = \begin{bmatrix} -1 & 0 & 0 & 0 & 0 & 0 \\ 0 & -1 & 0 & 0 & 0 & 0 \\ 0 & 0 & -1 & 0 & 0 & 0 \\ 0 & 0 & 0 & -1 & 0 & 0 \\ 0 & 0 & 0 & 0 & -1 & 0 \\ 0 & 0 & 0 & 0 & 0 & -1 \end{bmatrix}$$

and

$$Q_{12(k+1)} = \begin{bmatrix} -3(k+1)-1 & 0 & 0 & 0 & 3(k+1) & 0 \\ 0 & -3(k+1)-1 & 0 & 0 & 0 & 3(k+1) \\ -3(k+1) & 0 & -1 & 0 & 3(k+1) & 0 \\ 0 & -3(k+1) & 0 & -1 & 0 & 3(k+1) \\ -3(k+1) & 0 & 0 & 0 & 3(k+1)-1 & 0 \\ 0 & -3(k+1) & 0 & 0 & 0 & 3(k+1)-1 \end{bmatrix}.$$

$\square$

Knowing the c-matrices, we can compute the minimal weight for each cluster variable x_i.

4.2 Minimal Matching

Since D'_n and $D'_{n+1/2}$ are rotations of D_n and $D_{n+1/2}$, we will mainly work with D_n and $D_{n+1/2}$ only.

Let the *zero line* be the horizontal line passing through the starting point of the contour, we will consider the following perfect matching.

- For the edges on and above the 0 level, match all $1-6, 5-4, 2-3$ edges.
- For the edges below the 0 level, match all $1-4, 2-5, 3-6$ edges (except the $2-6$ dangling edge in $D_{n+1/2}$).

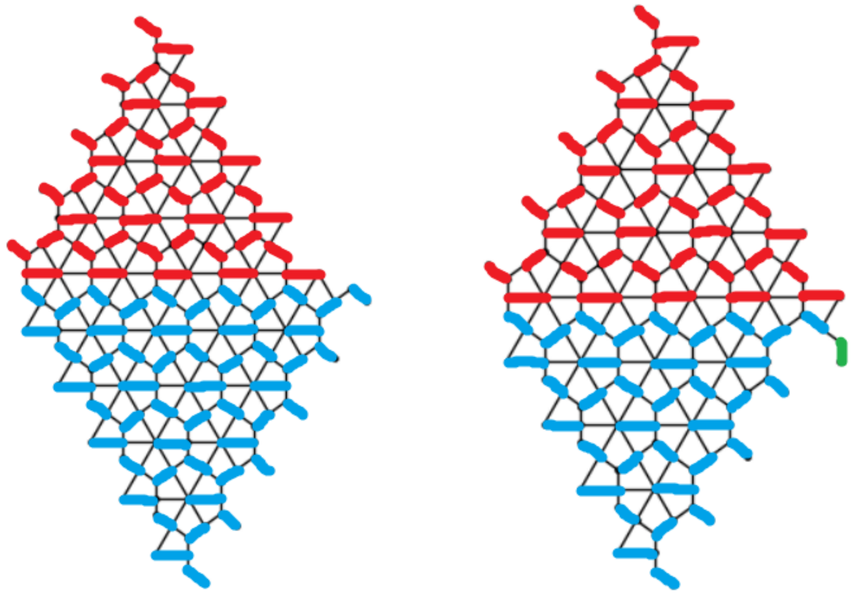

(a) Minimal matching of D_5 (b) Minimal matching of $D_{4+1/2}$

Proposition 4.2. *The above perfect matching is the unique minimal matching.*

Proof. We will prove this using Kuo condensation. By the discussion in Section 3, we choose four points A, B, D, E as shown in figures 23 and 24. As can be seen in the figures, from a Dragon D_i removing all four points A, B, D, E gives the Dragon $D_{i-3/2}$ while removing pairs of two points give $D_{i-1}, D_{i-1/2}, D'_{i-1}, D'_{i-1/2}$.

The c-matrices in Lemma 4.1 tell us that

$$z_{0,n,1}z_{-1,n-1,0} = z_{0,n-1,1}z_{-1,n,0} + \prod y_i z_{0,n-1,0}z_{-1,n,1}$$
$$z_{-1,n+1,0}z_{0,n-1,1} = z_{0,n,1}z_{-1,n,0} + \prod y_i z_{0,n,0}z_{-1,n,1}$$

In both cases, we can see that superimposing D_i and $D_{i-3/2}$ gives the same double dimer cover as superimposing D_{i-1} and $D_{i-1/2}$. On the other hand, superimposing D'_{i-1} and $D'_{i-1/2}$ gives the product of y_i that matches the above two equations. This verifies that the proposed perfect matching satisfies the recurrence for Aztec Dragons, and hence proves that it is indeed the minimal matching. □

Now we demonstrate how the minimal weight can be easily computed from the minimal matching.

Lemma 4.3. *For $dP3$ quiver, the minimal weight of a cluster variable x_i, denoted as $mon(x_i)$, is:*

$$mon(x_{4k}) = \frac{x_4 x_6^k}{x_2^k}, \quad mon(x_{4k+1}) = \frac{x_5^k}{x_1^{k-1}}, \quad mon(x_{4k+2}) = \frac{x_6^k}{x_2^{k-1}}, \quad mon(x_{4k+3}) = \frac{x_3 x_5^k}{x_1^k}.$$

Proof. Since for each region above and below the zero line, we use the same matching pattern, every face in each region has exactly one edge, and so does not contribute to the weight. Thus, to compute the weight, we only need to consider the faces along the zero line.

In the case of D_n, we have exactly n faces 5 having no edge, and exactly $n-1$ faces 1 having two edges. Therefore, the weight of the perfect matching is $\dfrac{x_5^n}{x_1^{n-1}}$.

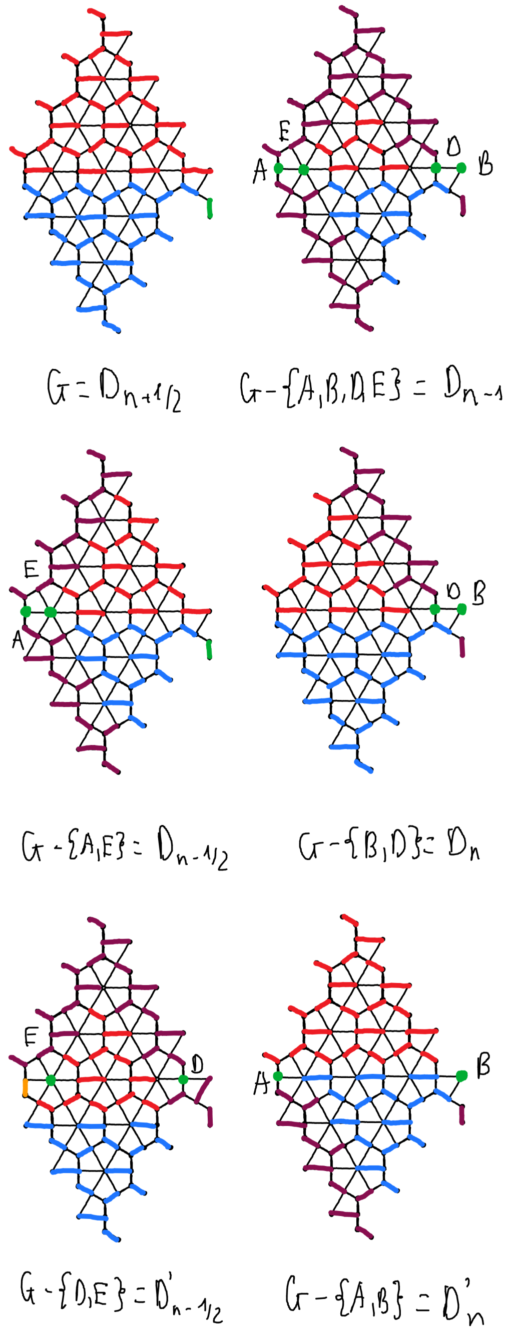

Figure 23: Kuo condensation for $D_{n+1/2}$

In the case of $D_{n+1/2}$, we have exactly n faces 5 having no edge, exactly n faces 1 having two edges, and one face 3 having no edge at the $2-6$ dangling edge. Therefore, the weight of the perfect matching is $\dfrac{x_3 x_5^n}{x_1^n}$.

$\square$

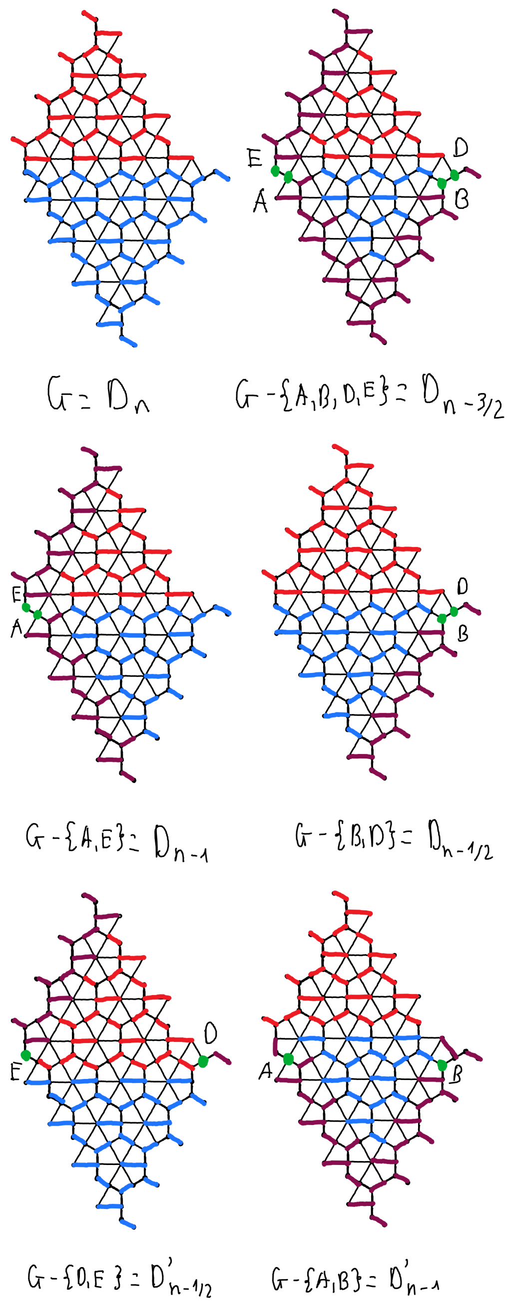

Figure 24: Kuo condensation for D_n

Remark. We can also verify these minimal weights by checking that the g-matrix formed by these weights, together with the c-matrix found in Lemma 4.1, satisifies Theorem 2.2.

5 Minimal matching of Aztec Castles

Now we give the minimal matching for Aztec Castles. In general, the construction is more complicated than for Aztec Dragons since we now vary all i, j, k in all direction.

5.1 Construction

In this section, we will give the construction of the minimal matching, which will be proved later in Section 6. Specifically, we will give the construction for generic cases when none of the sides is 0. The construction has two main steps.

- *Step 1: Dividing the Castle into regions.* We transverse along the sides of the contour in clockwise direction. At each corner, we perform one of the following actions:
  - If we move from a positive side to a positive side, draw a straight line in the direction of the second side.
  - If we move from a negative side to a negative side, draw a straight line in the direction of the first side.
  - If we move from a negative side to a positive side, draw a staircase diagonally, with the first step lying on the positive side.
  - If we move from a positive side to a negative side, no action is required.

  Since the tuple for the Castle does not alternate in sign, there are exactly two straight lines and two staircases. Also, by checking every case, we found that these two straight lines and two staircases intersect at two points (one per pair of line a staircase), and the two points can be connected by a straight line. We connect these two points by that straight line, and we call this line the *zero line*. This is because this line is the zero line in the Aztec Dragon case.

  After this step, the Castle is divided into four regions, two of them are each incident to one side of the contour while the other two are each incident to two sides. The four regions for all possible Castle shapes can be seen in Figure 25.

- *Step 2: Covering each region according to the side.* We will use a universal covering for each region, and the covering is determined by the side of the contour that the region is incident to as in Table 1.

Side	Positive	Negative
a	$1-4, 2-5, 3-6$	$1-5, 2-4, 3-6$
b	$1-4, 2-6, 3-5$	$1-4, 2-5, 3-6$
c	$1-3, 2-6, 4-5$	$1-4, 2-6, 3-5$
d	$1-6, 2-3, 4-5$	$1-3, 2-6, 4-5$
e	$1-5, 2-3, 4-6$	$1-6, 2-3, 4-5$
f	$1-5, 2-4, 3-6$	$1-5, 2-3, 4-6$

Table 1: Universal covering for each case

Note that in Table 1, the matching when one side is positive is the same as when the next side is negative. This is because in step 1, when moving from a positive side to a negative side, we do nothing, so these two sides are incident to the same region. Thus, they should have the same universal covering. Also when two consecutive sides have the same sign, their universal covering has one edge in common. This means that there is a "smooth transition" between the two corresponding regions. As a result, when considering the weight of this matching, the nonzero terms do not come from faces along the straight line dividing the two regions. The nonzero terms also do not come from faces in the interior of each region either. Therefore, the nonzero terms only come from faces along the two staircases and the zero line. This allows for easy calculations of the minimal weight of this matching.

Remark. There seems to be a small ambiguity in step 2 above for the covering on the zero line as we may have the choice of which covering to use. However, depending on the parity of the staircases' length, there is only a unique choice for this line.

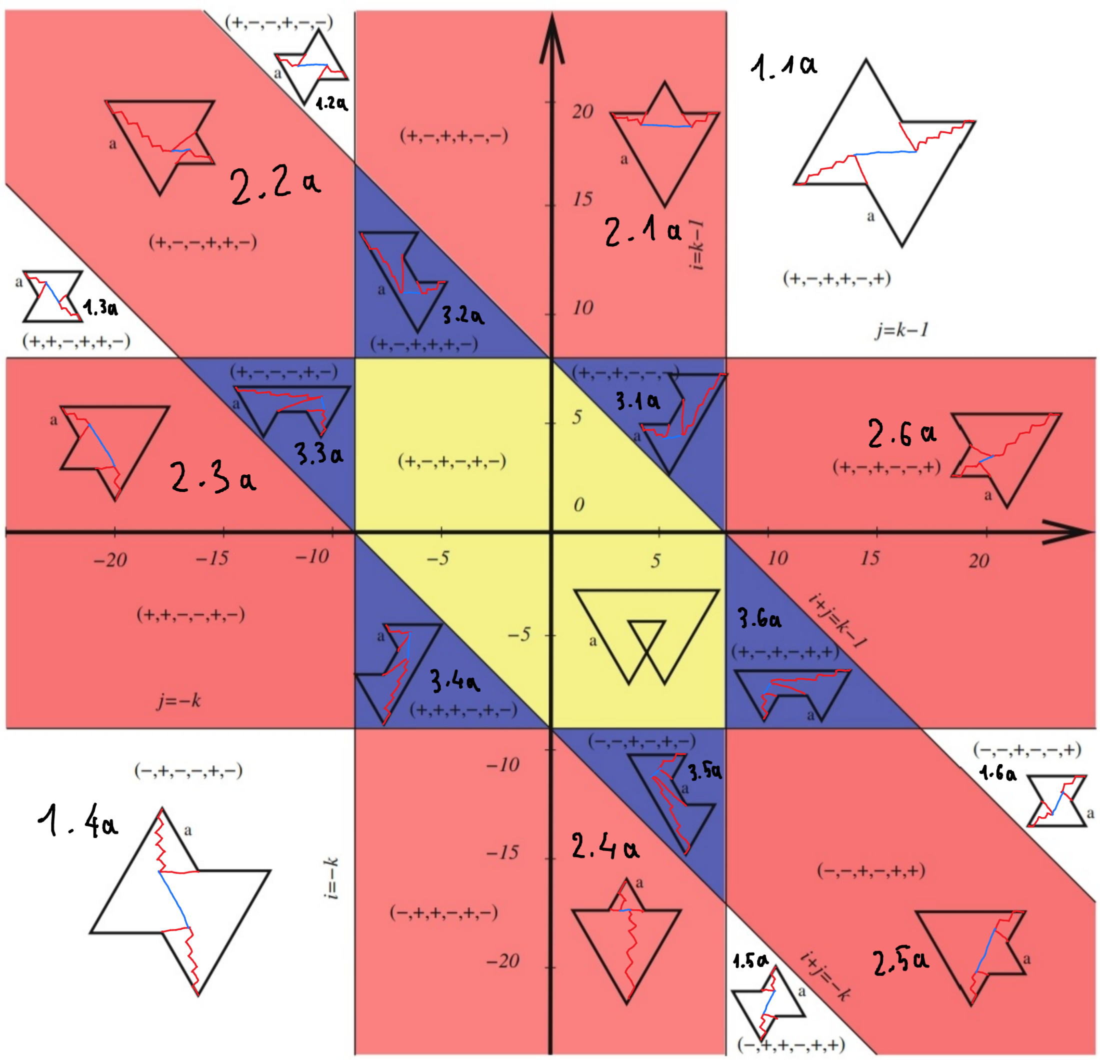

Figure 25: Four regions in each possible Castle shape

Figures 26, 27 and 28 show the four regions and minimal matchings of three Castles corresponding to three main families. Figure 29 shows the degenerate case when the f side is zero, which is the intersection of case 2.1a and 1.1a. Figure 30 shows the degenerate case when sides d and f are zero. Finally, figure 31 and 32 show how the regions change from case 2.1a to 1.1a, when the f side changes from negative to zero to positive, and how the regions change from a contour with one zero to a contour with two zeros.

Figure 33 shows how the weight of the minimal matching can be calculated easily. The purple faces

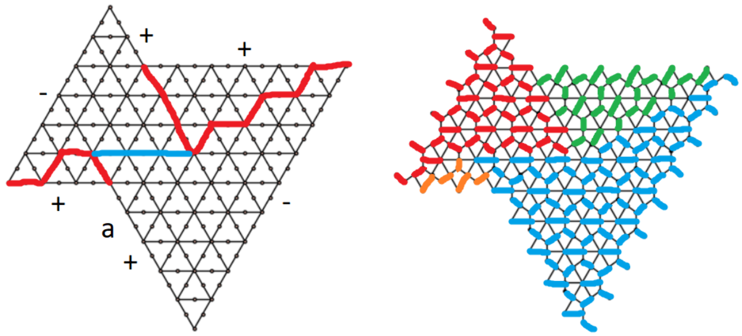

(a) Four regions (b) Minimal matching

Figure 26: Four regions and minimal matching of Castle $C_{4,3,2}$ in case 1.1a

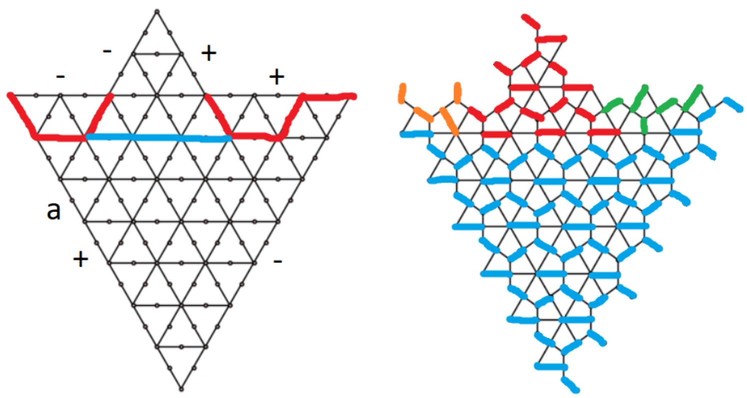

(a) Four regions (b) Minimal matching

Figure 27: Four regions and minimal matching of Castle $C_{0,4,3}$ in case 2.1a

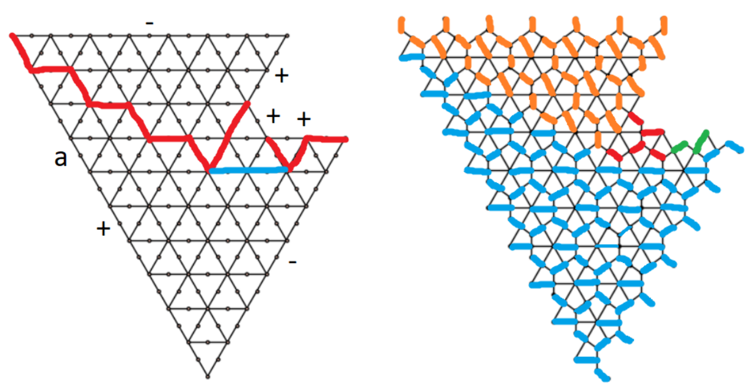

(a) Four regions (b) Minimal matching

Figure 28: Four regions and minimal matching of Castle $C_{-3,5,5}$ in case 3.2a

are the only faces with zero or two edges, and so they are the only faces contributing to the weight. Notice that these faces are all on the staircases and the zero line.

We are now ready to state our main theorem.

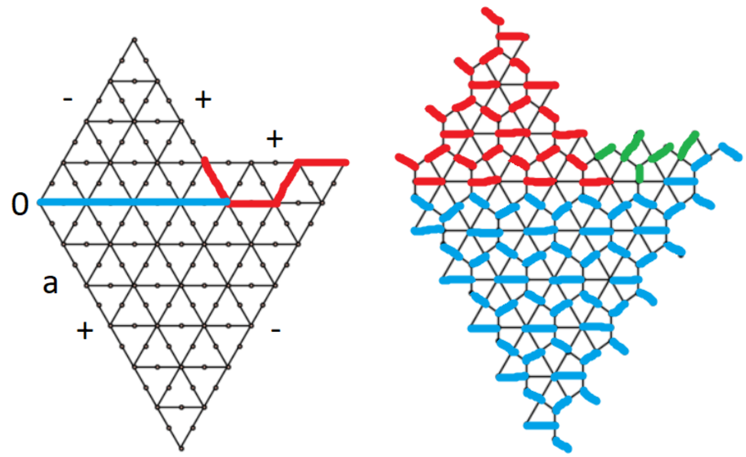

(a) Four regions (b) Minimal matching

Figure 29: Four regions and minimal matching of Castle $C_{1,4,2}$ in the intersection of 1.1a and 2.1a

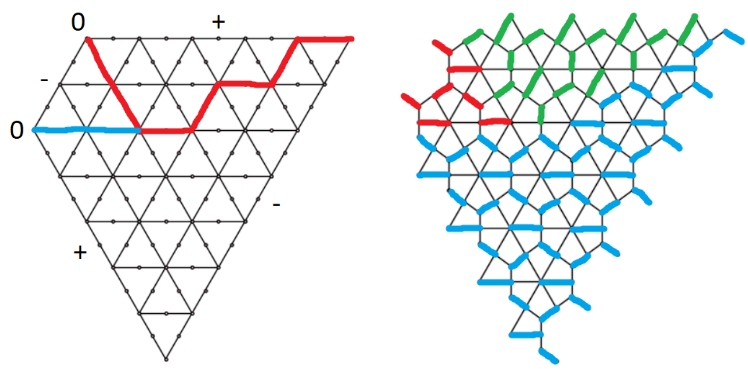

(a) Four regions (b) Minimal matching

Figure 30: Four regions and minimal matching of Castle $C_{2,2,3}$ where the contour has two zeros

Theorem 5.1. *The above construction gives the minimal matching of any Aztec Castles.*

5.2 Minimal weight

Before proving the main theorem, we will show that the weight of the proposed perfect matching can be easily calculated with examples from region 1.1a.

Let $i = k - 1 + m$ and $j = k - 1 + n$ where $m, n > 0$, we have two cases.

- *Case 1:* If $m = 2p$, then the contour is

$$(k + j, j + k + i, 2(k - 1 + p) + 1, n, n + i, 2p).$$

Thus, the staircase on side c has height $k - 1 + p$, and the staircase on side f has height p. This means that the first staircase contributes $x_3^{-(k-1+p)} x_5^{k-1+p}$ and the second staircase contributes $x_4^{-p} x_6^{p}$. We can also see that the zero line has length $n + k - 1$, which means this contributes $x_1^{-(n+k-1)} x_5^{n+k}$ to the weight. Thus, the weight of the perfect matching is

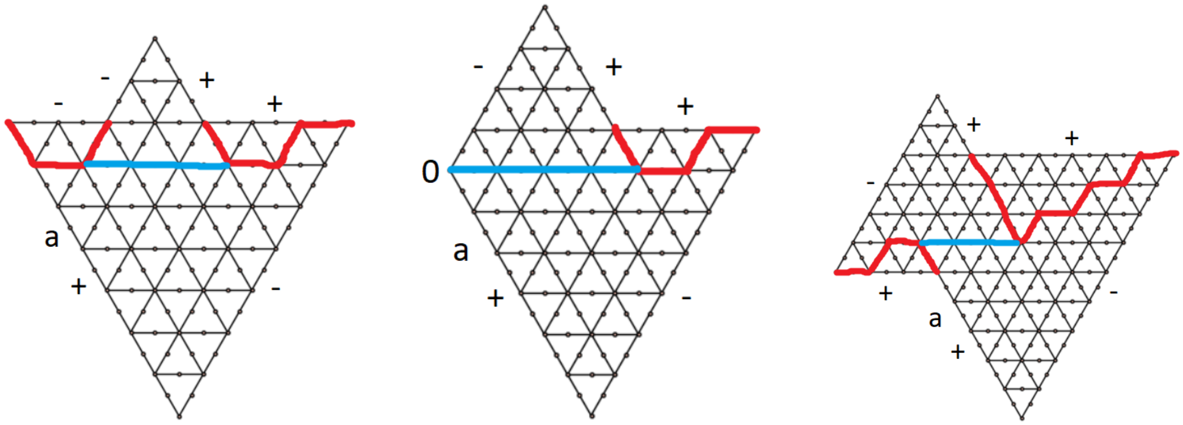

(a) 2.1a (b) Intersection (c) 1.1a

Figure 31: Transition from 2.1a to 1.1a, where the f side changes from negative to zero to positive

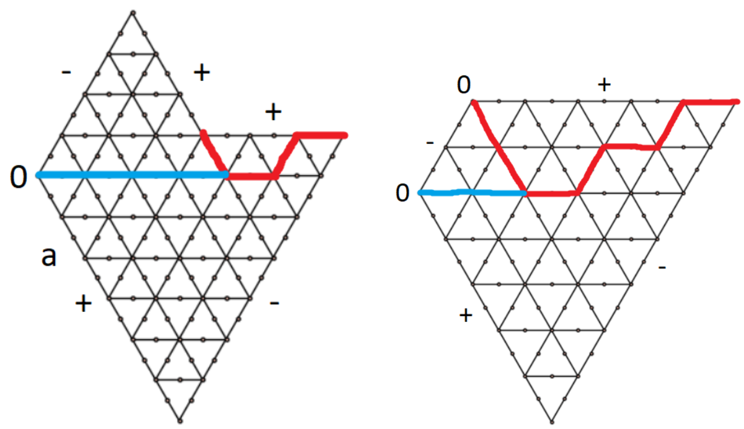

(a) One zero (b) Two zeros

Figure 32: Contour with one zero degenerates to contour with two zeros

$$\frac{x_5^{2k-1+p+n} x_6^p}{x_1^{n+k-1} x_3^{k-1+p} x_4^p}$$

- *Case 2:* If $m = 2p - 1$, then the contour is

$$(k + j, j + k + i, 2(k - 1 + p), n, n + i, 2p - 1).$$

Thus, the staircase on side c has height $k-1+p$, and the staircase on side f has height $p-1$. This means that the first staircase contributes $x_3^{-(k-1+p)} x_5^{k-1+p}$ and the second staircase contributes $x_4^{-(p-1)} x_6^{p-1}$. We can also see that the zero line has length $n+k-1$, which means this contributes $x_2^{-(n+k-1)} x_6^{n+k}$ to the weight. Thus, the weight of the perfect matching is

$$\frac{x_5^{k-1+p} x_6^{n+k+p-1}}{x_2^{n+k-1} x_3^{k-1+p} x_4^{p-1}}$$

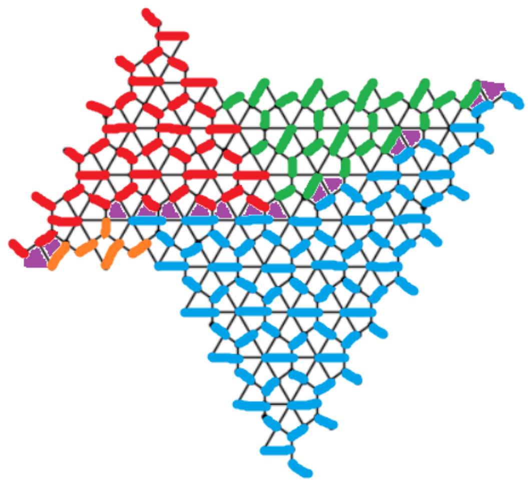

Figure 33: Weight of minimal matching of Castle $C_{4.3.2}$

A question may arise from the above reasoning is why the zero line contributes $x_1^{-(n+k-1)}x_5^{n+k}$ in one case and $x_2^{-(n+k-1)}x_6^{n+k}$ in the other. This is because of the canonical choice on the zero line that we have in the construction. Figure 34 illustrates this choice clearly. When m is even, the zero line follows the top region while when m is odd, it follows the bottom region.

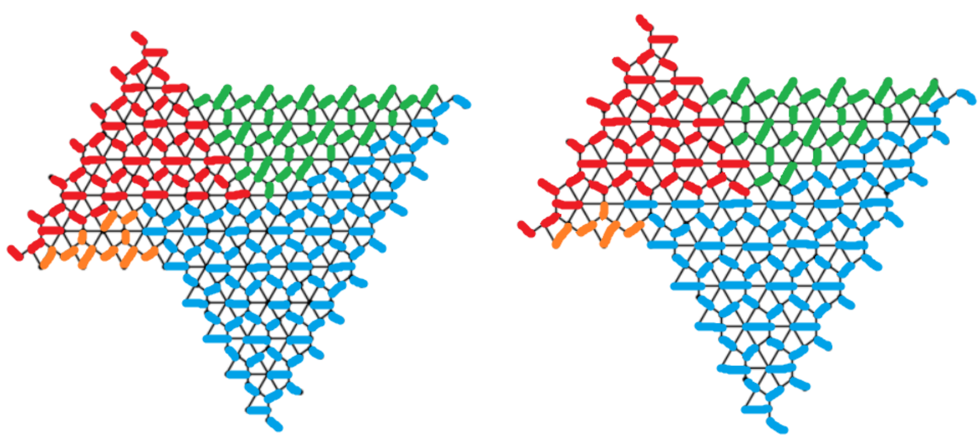

(a) even m

(b) odd m

Figure 34: Contour with one zero degenerates to contour with two zeros

6 Proof of main theorem

6.1 Recurrences

We will verify that the minimal matching satisfies the three types of recurrences described in [12]. These are

$(R4)$ $z_{i-1,j+2,k}z_{i,j,k+1} = z_{i-1,j+1,k}z_{i,j+1,k+1} + z_{i-1,j+1,k+1}z_{i,j+1,k}$

$(R1)$ $z_{i-1,j+1,k+1}z_{i,j+1,k-1} = z_{i-1,j+2,k}z_{i,j,k} + z_{i-1,j+1,k}z_{i,j+1,k}$

$(R2)$ $z_{i-1,j+2,k}z_{i+1,j,k} = z_{i,j+1,k-1}z_{i,j+1,k+1} + z^2_{i,j+1,k}$

The three types are illustrated in Figure 35.

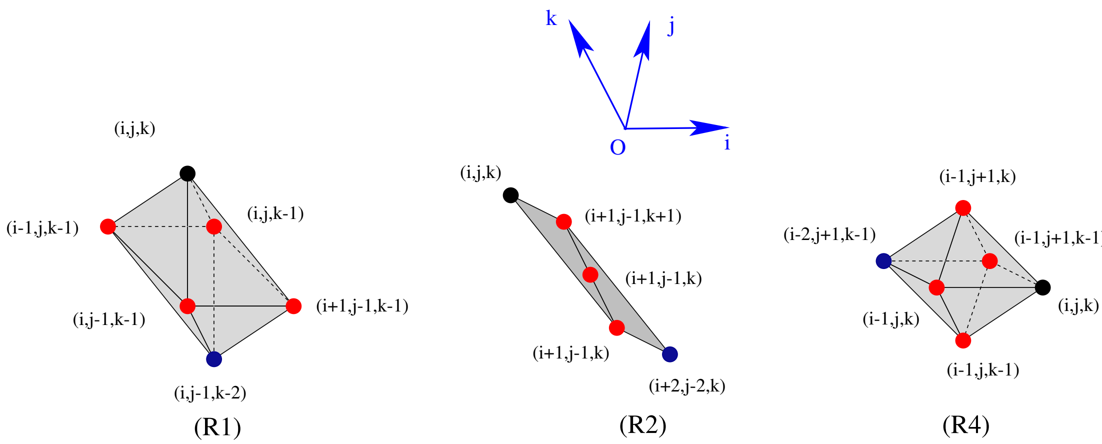

Figure 35: Three types of recurrences, source: [12]

The $(R4)$ recurrences correspond to replacing the cluster variable $z_{i,j,k}$ with one of twelve possibilities:

$$z_{i-1,j+2,k\pm1}, \quad z_{i+1,j-2,k\pm1}, \quad z_{i+2,j-1,k\pm1}, \quad z_{i-2,j+1,k\pm1}, \quad z_{i-1,j-1,k\pm1}, \quad z_{i+1,j+1,k\pm1}.$$

In terms of the 6-tuples, this corresponds to replacing (a,b,c,d,e,f) with

$$(a-2, b+3, c-2, d, e-1, f)$$

or a cyclic rotation or negation of this transformation. As described in Section 3, this corresponds to choosing A, B, C, E, or its cyclic rotation.

The $(R1)$ recurrences correspond to replacing the cluster variable $z_{i,j,k}$ with one of twelve possibilities:

$$z_{i+1,j,k\pm2}, \quad z_{i-1,j,k\pm2}, \quad z_{i,j+1,k\pm2}, \quad z_{i,j-1,k\pm2}, \quad z_{i+1,j-1,k\pm2}, \quad z_{i-1,j+1,k\pm2}.$$

In terms of the 6-tuples, this corresponds to replacing (a,b,c,d,e,f) with

$$(a+3, b-2, c+1, d-1, e+2, f-3)$$

or a cyclic rotation or negation of this transformation. As described in Section 3, this corresponds to choosing A, B, E, F, or its cyclic rotation.

The $(R2)$ recurrences correspond to replacing the cluster variable $z_{i,j,k}$ with one of twelve possibilities:

$$z_{i+2,j,k}, \quad z_{i-2,j,k}, \quad z_{i,j+2,k}, \quad z_{i,j-2,k}, \quad z_{i+2,j-2,k}, \quad z_{i-2,j+2,k}.$$

In terms of the 6-tuples, this corresponds to replacing (a,b,c,d,e,f) with

$$(a, b+2, c-2, d, e+2, f-2)$$

or a cyclic rotation or negation of this transformation. As described in Section 3, this corresponds to choosing B, C, E, F, or its cyclic rotation.

We will use Kuo condensation to prove that the minimal matching satisfies the three recurrences. We will prove this in detail in Section 6.3. Generally, the main point of the proof is to compare the staircase regions in the matching and show that after superimposing, they are similar. In this report, we will show the details for case 1.1, and other regions can be shown analogously.

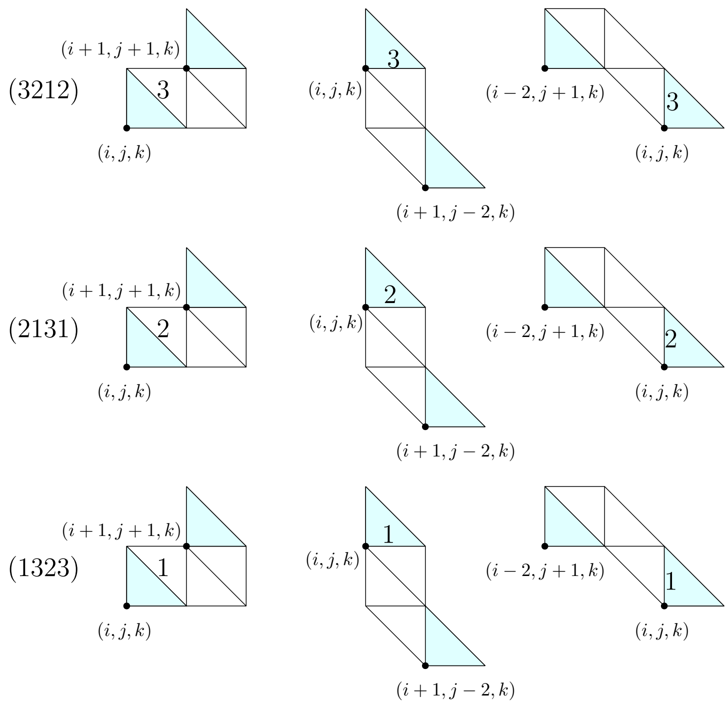

Figure 36: Action of m_1, m_2, m_3 on the (i,j) position of prisms

6.2 c-matrix

Before continuing with Kuo condensation, we will prove an important property of the c-matrix.

Lemma 6.1. *When the prism has its bottom right angle position at (i,j,k), the mutation sequences $(\tau_3\tau_2\tau_1\tau_2)$, $(\tau_2\tau_1\tau_3\tau_1)$, $(\tau_1\tau_3\tau_2\tau_3)$, and each of their infinite products preserve the sign of each column in the $c-$vector.*

Proof. Since the position of prism is fixed for each (i,j,k), $m_1 = (\tau_3\tau_2\tau_1\tau_2)$, $m_2 = (\tau_2\tau_1\tau_3\tau_1)$, and $m_3 = (\tau_1\tau_3\tau_2\tau_3)$ move the prism in the same way with different starting positions. Call the starting edge of each m_i mutation, $m_i(1)$ (e.g. $m_1(1) = 3$, $m_2(1) = 2$, $m_3(1) = 1$). Observe that all m_i move the prism from (i,j,k) to $(i+1,j+1,k)$ if $m_i(1)$ is the diagonal side, (i,j,k) to $(i+1,j-2,k)$ if $m_i(1)$ is the horizontal edge of the triangle, and (i,j,k) to $(i-2,j+1,k)$ if $m_i(1)$ is the vertical edge. Also, m_i position the prism the same way as it did before the mutation. In other words, if $m_i(1)$ were on the diagonal side, it remains to be on the diagonal side. Then by induction, we can show the sign preserved property. Without loss of generality, we only consider m_1 and fix $k = 1$ below to consider the base case.

This is a work in progress. □

Lemma 6.2. *When the prism has its bottom right angle position at (i,j,k), the mutation sequence τ_5, τ_4, and their alternating infinite product $(\tau_5\tau_4\dots)$ preserve the sign of each column in the $c-$vector.*

Proof. This is a work in progress. □

Proposition 6.3. *Consider the c-vector for each (i,j,k) in region 1.1, where the prism has its bottom* *right angle at (i,j,k). Then, the only negative columns of the c-vector at (i,j,k) are*

$$\begin{cases} \text{col } 1,2, & \text{when } i-j \equiv 1 \pmod 3 \\ \text{col } 3,4, & \text{when } i-j \equiv 2 \pmod 3 \\ \text{col } 5,6, & \text{when } i-j \equiv 0 \pmod 3 \end{cases}.$$

Proof. Since we position the prism in the same way for each position, the mutating sequence are predictable. Therefore, there are 6 cases to prove by induction.

- *Case 1* $(k-1,k-1,k)$: The base case is $(0,0,1)$, where we mutate the original prism through $\tau_2\tau_1\tau_2$ to get to the desired position. For our purpose, we do not consider if $\tau_2\tau_1\tau_2$ change the c-vectors are not since we always start our mutation sequence with $\tau_2\tau_1\tau_2$ in region 1.1. Here, the c-vector of $(0,0,1)$ is

$$\begin{pmatrix} 0 & 0 & 0 & 1 & -2 & 0 \\ 0 & 0 & 1 & 0 & 0 & -2 \\ 1 & 0 & 0 & 0 & -1 & -1 \\ 0 & 1 & 0 & 0 & -1 & -1 \\ 0 & 0 & 0 & 0 & -1 & 0 \\ 0 & 0 & 0 & 0 & 0 & -1 \end{pmatrix},$$

  having column 5 and 6 negative. Notice that the mutation sequence from $(k-1,k-1,k)$ to $(k,k,k+1)$ is $(\tau_3\tau_2\tau_1\tau_2\tau_4)$ if k is even and $(\tau_3\tau_2\tau_1\tau_2\tau_5)$ if k is odd. Given k, assume that $(k-1,k-1,k)$ also has column 5 and 6 as negative columns. Since τ_4, and τ_5 all preserve the signs of each column, by induction, $(k,k,k+1)$ also has column 5 and 6 negative.

- *Case 2* (n,n,k): The base case is Case 1, whose negative columns are always column 5 and 6. Assume that the negative columns are always 5 and 6 for $(i,j,k) = (n-1,n-1,k)$, where $n > k$. Note that the mutation sequence from $(n-1,n-1,k)$ to (n,n,k) is $(\tau_3\tau_2\tau_1\tau_2), \forall n > k$. Since $(\tau_3\tau_2\tau_1\tau_2)$ preserves the sign of columns, by induction, the negative columns are always 5 and 6 for (n,n,k) as desired.

- *Case 3* $(k-1,j,k)$: When $j = k-1$, this is reduced to Case 1. Fix $k = 1$, for $j > k-1$, from $(k-1,j,1)$ to $(k-1,j+1,1)$, we mutate

$$\begin{cases} (\tau_3\tau_1), & \text{for } j \equiv 0 \pmod 3 \\ (\tau_2\tau_3), & \text{for } j \equiv 1 \pmod 3 \\ (\tau_1\tau_2), & \text{for } j \equiv 2 \pmod 3 \end{cases}.$$

  Then, as we increase $k > 1$, we mutate

$$\begin{cases} (\tau_2\tau_1\tau_3\tau_1), & \text{for } j-k \equiv 0 \pmod 3 \\ (\tau_1\tau_3\tau_2\tau_3), & \text{for } j-k \equiv 1 \pmod 3 \\ (\tau_3\tau_2\tau_1\tau_2), & \text{for } j-k \equiv 2 \pmod 3 \end{cases}.$$

  Note the c-vectors for $(0,1,1)$ and $(0,2,1)$ respectively are

$$\begin{pmatrix} 2 & 0 & 0 & -3 & 0 & 0 \\ 0 & 2 & -3 & 0 & 0 & 0 \\ 1 & 0 & -1 & -2 & 1 & 0 \\ 0 & 1 & -2 & -1 & 0 & 1 \\ 1 & 0 & 0 & -2 & 0 & 0 \\ 0 & 1 & -2 & 0 & 0 & 0 \end{pmatrix} \quad \text{and} \quad \begin{pmatrix} -4 & 0 & 0 & 0 & 3 & 0 \\ 0 & -4 & 0 & 0 & 0 & 3 \\ -3 & -1 & 0 & 1 & 2 & 0 \\ -1 & -3 & 1 & 0 & 0 & 2 \\ -3 & 0 & 0 & 0 & 2 & 0 \\ 0 & -3 & 0 & 0 & 0 & 2 \end{pmatrix},$$

having column 3 and 4 negative and column 1 and 2 negative. Also, $(0,0,1)$ in Case 1 has negative columns 5 and 6. Then, since $(\tau_2\tau_1\tau_3\tau_1)$, $(\tau_1\tau_3\tau_2\tau_3)$, $(\tau_3\tau_2\tau_1\tau_2)$, (τ_4) and (τ_5) preserve the sign of each column for the c-vectors, if we assume that $(k-1,j,k)$ satisfies the proposition, then the induction cases for $(k-1,j+1,k)$ follows.

- *Case 4* $(i,k-1,k)$: This is similar to Case 3. When $i=k-1$, this is reduced to Case 1. Fix $k=1$, for $i>k-1$, from $(i,k-1,1)$ to $(i+1,k-1,1)$, we mutate

$$\begin{cases} (\tau_3\tau_2), & \text{for } j \equiv 0 \pmod 3 \\ (\tau_1\tau_3), & \text{for } j \equiv 1 \pmod 3 \\ (\tau_2\tau_1), & \text{for } j \equiv 2 \pmod 3 \end{cases}.$$

Then, as we increase $k>1$, we mutate

$$\begin{cases} (\tau_1\tau_3\tau_2\tau_3), & \text{for } j-k \equiv 0 \pmod 3 \\ (\tau_2\tau_1\tau_3\tau_1), & \text{for } j-k \equiv 1 \pmod 3 \\ (\tau_3\tau_2\tau_1\tau_2), & \text{for } j-k \equiv 2 \pmod 3 \end{cases}.$$

along with τ_4 if k is even and τ_5 k is odd. Note the c-vectors for $(1,0,1)$ and $(2,0,1)$ respectively are

$$\begin{pmatrix} -1 & -2 & 1 & 0 & 0 & 1 \\ -2 & -1 & 0 & 1 & 1 & 0 \\ -1 & -2 & 1 & 1 & 0 & 0 \\ -2 & -1 & 1 & 1 & 0 & 0 \\ -1 & -1 & 1 & 0 & 0 & 0 \\ -1 & -1 & 0 & 1 & 0 & 0 \end{pmatrix} \quad \text{and} \quad \begin{pmatrix} 1 & 0 & -1 & -3 & 1 & 1 \\ 0 & 1 & -3 & -1 & 1 & 1 \\ 0 & 0 & -2 & -2 & 2 & 1 \\ 0 & 0 & -2 & -2 & 1 & 2 \\ 0 & 0 & -1 & -2 & 1 & 1 \\ 0 & 0 & -2 & -1 & 1 & 1 \end{pmatrix},$$

having column 1 and 2 negative and column 3 and 4 negative. Also, $(0,0,1)$ in Case 1 has negative columns 5 and 6. Then, since $(\tau_2\tau_1\tau_3\tau_1)$, $(\tau_1\tau_3\tau_2\tau_3)$, $(\tau_3\tau_2\tau_1\tau_2)$, (τ_4) and (τ_5) preserve the sign of each column for the c-vectors, if we assume that $(k-1,j,k)$ satisfies the proposition, then the induction cases for $(k-1,j+1,k)$ follows.

- *Case 5* (n,j,k): Apply the mutation sequences in Case 4 to Case 3 (base case) to prove the proposition from $(k-1,j,k)$ to (n,j,k) by induction.

- *Case 6* (i,n,k): Apply the mutation sequences in Case 3 to Case 4 (base case) to prove the proposition from $(i,k-1,k)$ to (i,n,k) by induction.

□

6.3 Kuo Condensation

As discussed in Section 6.1, we only need to show that the proposed perfect matching satisfies the three recurrences $(R4),(R1),(R2)$.

We will first verify the minimal matching for the $(R4)$ recurrence when replacing $z_{i-1,j-1,k-1}$ by $z_{i,j,k}$. Let G be the Castle $C_{i,j,k}$, then by the discussion in Section 6.1, we will choose four points A,B,C,E. We have the following graphs for each case of deletion:

Points removed	Resulting Castle
A, B, C, E	$C_{i-1,j-1,k-1}$
A, B	$C_{i,j-1,k-1}$
C, E	$C_{i-1,j,k}$
A, E	$C_{i,j-1,k}$
B, C	$C_{i-1,j,k-1}$

By the sign pattern in Section 6.2, the cluster mutation corresponding to these vertices is

$$z_{i-1,j-1,k-1}z_{i,j,k} = z_{i,j-1,k}z_{i-1,j,k-1} + \left(\prod_i y_i\right) z_{i,j-1,k-1}z_{i-1,j,k}.$$

This means that we only need to compare the superimposing of G and $G-\{A,B,C,E\}$ with $G-\{A,E\}$ and $G-\{B,C\}$. Figure 37 shows this comparison, where the staircases and zero line match perfectly.

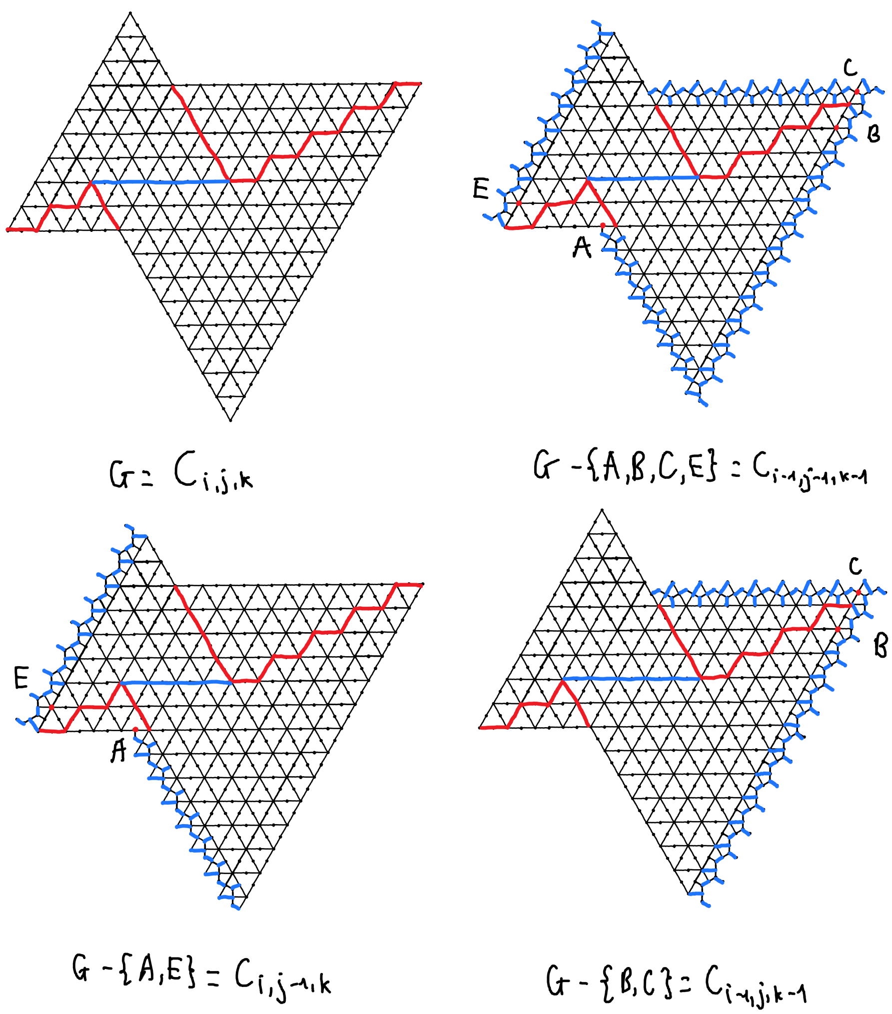

Figure 37: Kuo condensation for $(R4)$

Verifying the minimal matching for the $(R2)$ recurrence when replacing $z_{i-2,j,k}$ by $z_{i,j,k}$ works similarly. Let G be the Castle $C_{i,j,k}$, then by the discussion in Section 6.1, we will choose four points B, C, E, F. We have the following graphs for each case of deletion:

Points removed	Resulting Castle
B, C, E, F	$C_{i-2,j,k}$
B, C	$C_{i-1,j,k-1}$
E, F	$C_{i-1,j,k+1}$
C, E	$C_{i-1,j,k}$
B, F	$C_{i-1,j,k}$

By the sign pattern in Section 6.2, the cluster mutation corresponding to these vertices is

$$z_{i-2,j,k}z_{i,j,k} = z_{i-1,j,k-1}z_{i-1,j,k+1} + \left(\prod_i y_i\right) z_{i-1,j,k}^2.$$

This means that we only need to compare the superimposing of G and $G - \{B, C, E, F\}$ with $G - \{E, F\}$ and $G - \{B, C\}$. Figure 38 shows this comparison, where the staircases and zero line match perfectly.

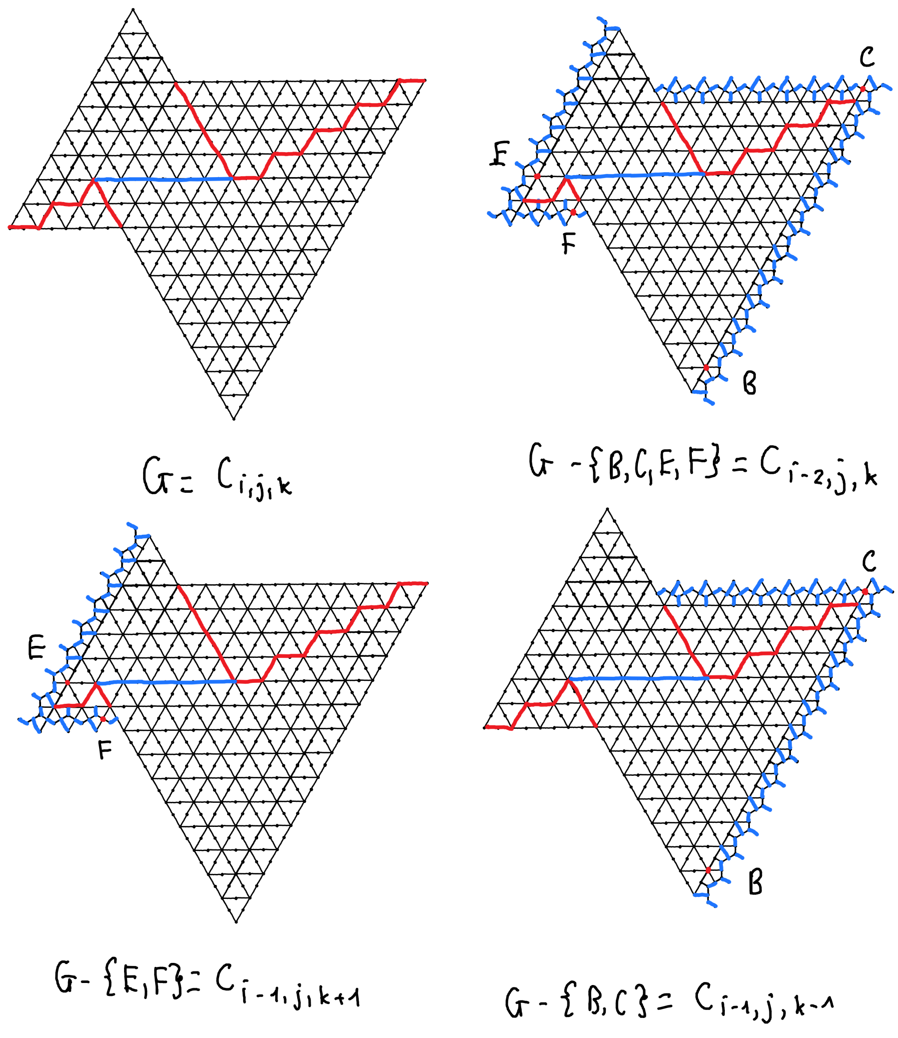

Figure 38: Kuo condensation for $(R2)$

Finally, we will verify the minimal matching for the $(R1)$ recurrence when replacing $z_{i+1,j-1,k-2}$ by $z_{i,j,k}$. For this recurrence, we will use the non-alternating version of Kuo condensation. Let G be the Castle $C_{i+1,j,k-1}$, then by the discussion in Section 6.1, we will choose four points A, B, E, F. We have the following graphs for each case of deletion:

Points removed	Resulting Castle
A, B, E, F	$C_{i,j-1,k-1}$
A, B	$C_{i+1,j-1,k-2}$
E, F	$C_{i,j,k}$
A, E	$C_{i+1,j-1,k-1}$
B, F	$C_{i,j,k-1}$

By the sign pattern in Section 6.2, the cluster mutation corresponding to these vertices is

$$z_{i+1,j-1,k-2}z_{i,j,k} = z_{i,j-1,k-1}z_{i+1,j,k-1} + \left(\prod_i y_i\right) z_{i+1,j-1,k-1}z_{i,j,k-1}.$$

This means that we only need to compare the superimposing of G and $G-\{A,B,E,F\}$ with $G-\{E,F\}$ and $G-\{A,B\}$. Figure 39 shows this comparison, where the staircases and zero line match perfectly.

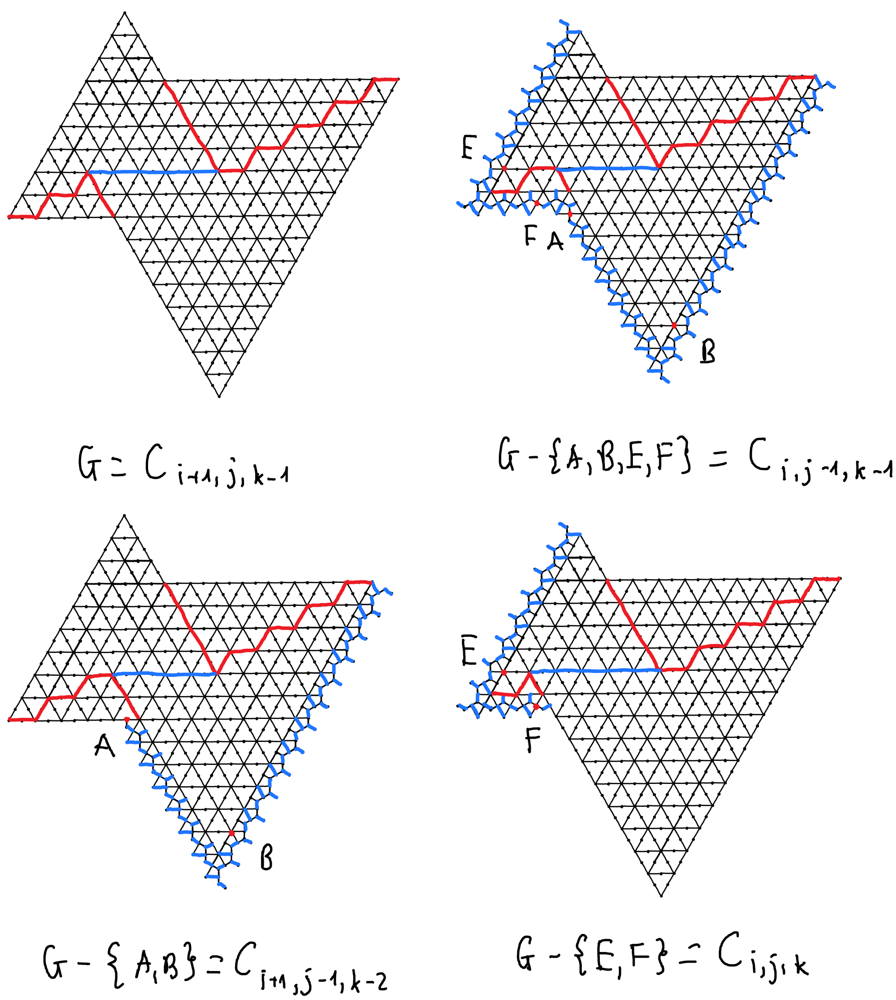

Figure 39: Kuo condensation for $(R1)$

Acknowledgements

This project was partially supported by RTG grant NSF/DMS-1745638. It was supervised as part of the University of Minnesota School of Mathematics Summer 2022 REU program. The authors would like to thank Gregg Musiker for his wonderful mentorship and for introducing the problem to us. The authors would also like to thank Carolyn Stephen and Sylvester Zhang for their continuous support throughout the project.

References

[1] Hanany A and Seong R, *Brane tilings and reflexive polygons*, **60** (2012).

[2] Keller B, *Cluster algebras, quiver representations and triangulated categories*, (2008).

[3] Mireille Bousquet-Mélou, James Propp, and Julian West, *Perfect matchings for the three-term gale-robinson sequences*, (2009).

[4] Cyndie Cottrell and Benjamin Young, *Domino shuffling for the del pezzo 3 lattice*, (2010).

[5] Speyer D and Williams L K, *The tropical totally positive grassmannian*, Journal of Algebraic Combinatorics **22** (2005).

[6] Harm Derksen, Jerzy Weyman, and Andrei Zelevinsky, *Quivers with potentials and their representations ii: applications to cluster algebras*, Journal of the American Mathematical Society **23** (2010), no. 3, 749–790.

[7] B. Feng, Y.-H. He, K. Kennaway, and C. Vafa, *Dimer models from mirror symmetry and quivering amoebae.*, **no. 3** (2008).

[8] Sergey Fomin and Andrei Zelevinsky, *Cluster algebras i: Foundations*, Journal of the American Mathematical Society **15** (2001), 497–529.

[9] Sergey Fomin and Andrei Zelevinsky, *Cluster algebras iv: Coefficients*, Compositio Mathematica **143** (2007), no. 1, 112–164.

[10] Mark Gross, Paul Hacking, Sean Keel, and Maxim Kontsevich, *Canonical bases for cluster algebras*, Journal of the American Mathematical Society **31** (2018), no. 2, 497–608.

[11] Eric H Kuo, *Applications of graphical condensation for enumerating matchings and tilings*, Theoretical Computer Science **319** (2004), no. 1-3, 29–57.

[12] Tri Lai and Gregg Musiker, *Beyond aztec castles: Toric cascades in the dp 3 quiver*, Communications in Mathematical Physics **356** (2017), no. 3, 823–881.

[13] Megan Leoni, Gregg Musiker, Seth Neel, and Paxton Turner, *Aztec castles and the dp3 quiver*, 2013.

[14] Tomoki Nakanishi and Andrei Zelevinsky, *On tropical dualities in cluster algebras*, Algebraic groups and quantum groups **565** (2012), 217–226.

[15] David E Speyer, *Perfect matchings and the octahedron recurrence*, (2004).

[16] Fock V V and Goncharov A B, *Moduli spaces of local systems and higher teichmuller theory*, Publications Mathematiques de IÍnstitut des Hautes Etudes Scientifiques **103** (2006).

[17] Sicong Zhang, *Cluster variables and perfect matchings of subgraphs of the* dp_3 *lattice*, 2015.